K. B. WINTERBON, PETER SIGMUND
AND J. B. SANDERS

SPATIAL DISTRIBUTION OF ENERGY DEPOSITED BY ATOMIC PARTICLES IN ELASTIC COLLISIONS

Synopsis

Energetic atomic particles slowing down in a solid or a gas create cascades of atomic collisions. This paper deals with the spatial distribution of the energy dissipated within the cascades, at the end of the slowing-down process. This distribution is of central interest in the theory of radiation damage and sputtering. An integro-differential equation determining the distribution function is derived under the assumption of random slowing down in an infinite medium. A set of equations is derived determining spatial moments over the distribution functions, and the moment equations are solved explicitly under the assumption of elastic scattering with power-law cross sections. The theory applies to heavy ions or recoil atoms in the keV range (for lighter ions only in the lower keV range), slowing down in a (monatomic or polyatomic) target under conditions where crystal lattice effects may be neglected. Moments over the distribution are tabulated for a wide range of mass ratios and several exponents in the Lindhard power cross section, and are compared to corresponding moments over the distribution of ion ranges. Several methods of constructing distributions from spatial moments are discussed, and some typical energy and range distributions are presented, both in one dimension (depth distribution) and three dimensions. A brief discussion of the experimental situation concludes the paper.

TABLE OF CONTENTS

1. Introduction

This is the first of a series of papers dealing with the spatial extension of radiation damage induced by energetic atomic particles bombarding a random target. The term radiation damage is used in a rather general sense to comprise a number of changes in physical properties that may be considered stable on a time scale determined by the slowing down of the primary particle, such as lattice defects, disordering, ionization, dissociation, etc. The bombarding particles may come from an external source such as ions from an accelerator, or from internal sources such as recoil atoms from radioactive decays or collisions caused by fast neutrons in a reactor. The targets may be gases, liquids, amorphous solids and, with some restrictions, crystalline solids.

Since radiation damage is a consequence of the deposition of the energy of the bombarding particle in the target, the spatial distribution of deposited energy is of primary interest for all damage effects that are proportional to the amount of energy deposited, and for emission phenomena like sputtering and secondary electron emission.

In general the energy of the primary particle will be shared between atoms and electrons of the target. It is necessary to separate these two contributions since the slowing-down behaviour of electrons and atoms is different. A further separation may have to be made when the target consists of more than one kind of atom.

In this first paper we deal with the comparatively simple case of a heavy ion or atom slowing down by binary elastic collisions, i.e. slow enough that the energy dissipated among electrons may be neglected as a first approximation. This is a useful starting point since many calculations can be performed by exact methods. The results should be appropriate for keV ions, the actual energy limit being determined by the atomic numbers of the ion and the target.

It turns out that the equations governing the spatial distribution of deposited energy are much like those determining the distribution of ion ranges. Both sets of equations can be solved by applying the same methods, and sometimes even the quantitative results are rather similar. We shall compare ion ranges and damage distributions extensively. One major reason is that very accurate measurements of range distributions have been done, while existing measurements of damage distributions suffer from various kinds of uncertainties.

The basic physical assumptions entering the theory are essentially those formulated by LINDHARD and his colleagues in a series of three papers published in this journal (LINDHARD et al., 1963 a, b, 1968). The mathematical formalism has been described in detail by one of us (SANDERS, 1968 a, b, 1969). Parts of the present work have been presented at a recent conference (SIGMUND & SANDERS, 1967), and some results have been utilized in more specific applications (SIGMUND et al., 1968; SIGMUND, 1968, 1969 a). In Section 2 we briefly summarize the scattering cross sections used in the present paper and discuss a zero order approximation to the damage distribution, based only on the specific energy loss. Integral equations determining energy distributions are derived in Section 3, and special care is taken to make the notation general enough to enable us to use the same equations under less restrictive assumptions. In Section 4 we consider equations determining moments over the damage distribution, and in Section 5 these equations are solved. While our previous calculations (SIGMUND & SANDERS, 1967) were done on a desk calculator, the present results were obtained by computer. This allows getting higher moments than previously and thus constructing distribution functions from the moments with more accuracy. Section 6 is devoted to this problem. Numerical results are presented in Section 7, and Section 8 contains a comparison with experimental and computer work.

2. Scattering & Stopping Cross Sections

Elastic Scattering

For screened Coulomb interaction between an ion and an atom or between two atoms LINDHARD et al. (1968) derived the following approximate form of the differential cross section:

$$d\sigma = \pi a^2 \frac{dt}{2\, t^{3/2}} f(t^{1/2}), \tag{1}$$

where

$$t = \varepsilon^2 T/T_m,$$
$$T_m = \gamma E,$$
$E = $ initial energy,
$T = $ recoil energy, $0 \leq T \leq T_m$,
$\gamma = 4M_1 M_2/(M_1 + M_2)^2$,
$M_1 = $ mass of scattered particle,
$M_2 = $ mass of recoiling particle,
$$\varepsilon = \left(\frac{M_2 E}{M_1 + M_2}\right)\left(\frac{Z_1 Z_2 e^2}{a}\right)^{-1},$$
$Z_1 = $ atomic number of scattered particle,
$Z_2 = $ atomic number of recoiling particle,
$a = $ screening radius,
$f(t^{1/2})$ is a function that depends on the assumed form of the screening function.

(1a)

The last two quantities are not accurately known. We shall follow LINDHARD et al. (1968) and use the screening radius

$$a = 0.8853 \, a_0 \, Z^{-1/3} \tag{2}$$

where

$$Z^{2/3} = Z_1^{2/3} + Z_2^{2/3}, \tag{2a}$$

$$a_0 = \hbar^2/me^2 = 0.529 \text{ Å}.$$

The function $f(t^{1/2})$ has been calculated for the collision of neutral Thomas-Fermi atoms. Fig. 1 shows Lindhard's $f(t^{1/2})$ together with an analytical approximation

$$f_A(t^{1/2}) = \lambda' t^{1/6}[1 + (2\lambda' t^{2/3})^{2/3}]^{-3/2}, \tag{3}$$

where

$$\lambda' = 1.309.$$

We determined λ' by least-squares fit to the numerical curve. It is seen that the two curves agree to well within the accuracy of the Thomas-Fermi approximation.

At small t eq. (3) goes over into $f(t^{1/2}) = \lambda' t^{1/6}$, which is a special case of the power approximation (LINDHARD et al., 1968)

$$f(t^{1/2}) = \lambda_m t^{1/2-m}. \tag{4}$$

Figure 1 also shows three examples of (4) for $m = 1/3$, $1/2$ and 1 with

$$\lambda_{1/3} = \lambda' = 1.309; \; \lambda_{1/2} = 0.327; \; \lambda_1 = 0.5. \tag{4a}$$

It is seen that the case $m = 1/3$ is an excellent approximation at small values of t, $m = 1/2$ is a reasonable over-all approximation, and $m = 1$ (Rutherford scattering) is appropriate for $t \gg 1$. In general (4) describes approximately the scattering from a potential of the form $V(r) \propto r^{-1/m}$.

In the following paragraphs we work only with the cross sections of (4) for several values of m since they allow simple analytic solution of the integral equations for range and damage distributions. From (1), (1a) and (4) we obtain
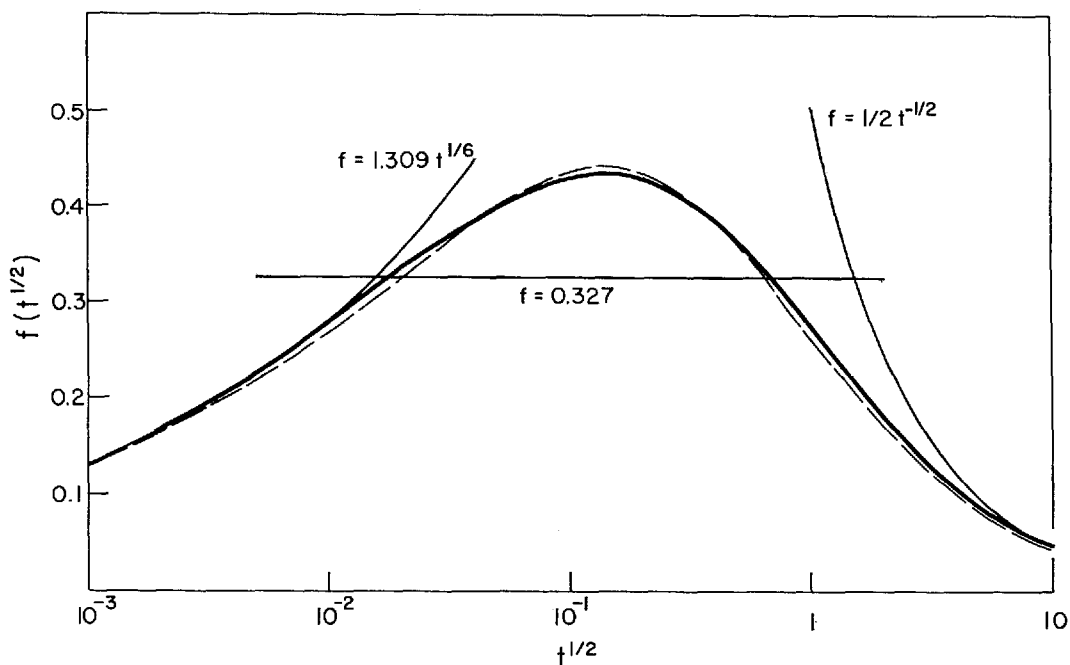
Fig. 1. Reduced Differential Cross Sections Calculated from Thomas-Fermi Potential. Thick solid line: Lindhard's numerical result. Dashed line: eq. (3). Thin solid lines: Power cross sections, eq. (4).

$$d\sigma = CE^{-m}T^{-1-m}dT, \tag{5}$$

where

$$C = \frac{\pi}{2}\lambda_m a^2 \left(\frac{M_1}{M_2}\right)^m \left(\frac{2Z_1Z_2e^2}{a}\right)^{2m}. \tag{5a}$$

Apart from the above three choices, we have made numerical calculations with $m = 2/3, 1/4, 1/8$, and $1/16$. While there is no specific energy region in Fig. 1 where any of these exponents would provide a particularly useful approximation to $f(t^{1/2})$ such calculations give an indication of how sensitive a quantity is to the shape of the differential cross section.

Calculations with the more accurate cross section (3) have also been performed. These can be done either analytically or numerically. In order that these results allow a more quantitative comparison with experiment than is possible on the basis of power cross sections it is necessary at the same time to include the effect of electronic energy loss. This work will be published separately.

To estimate the range of validity of the power cross sections it is convenient to consider the stopping cross section

$$S(E) = -\frac{1}{N}\frac{dE}{dR} = \int_0^{T_m} T d\sigma, \tag{6}$$
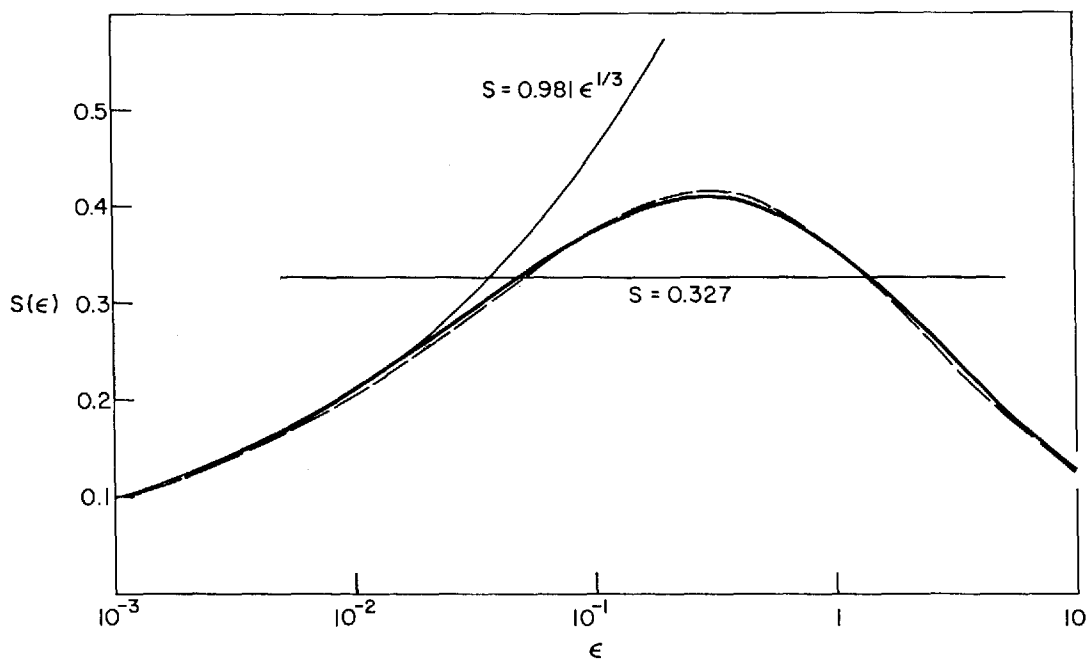
Fig. 2. Reduced Nuclear Stopping Cross Sections Calculated from Thomas-Fermi Potential. Thick solid line: Lindhard's numerical result. Dashed line: Integrated from eq. (3). Thin solid lines: eq. (10).

where dE/dR is the specific energy loss and N the density of atoms in the target, and the path length,

$$R(E) = \int_0^E \frac{dE}{NS(E)}. \tag{7}$$

In dimensionless units (LINDHARD et al. 1968), these read

$$s(\varepsilon) = -\frac{d\varepsilon}{d\varrho} = \frac{1}{\varepsilon} \int_0^\varepsilon f(t^{1/2}) dt^{1/2}, \tag{8}$$

and

$$\varrho(\varepsilon) = \int_0^\varepsilon \frac{d\varepsilon}{s(\varepsilon)}, \tag{9}$$

where

$$\varrho = RN\pi a^2 \gamma. \tag{9a}$$

Fig. 2 compares Lindhard's numerical curve with the one following from (3) by integration and the power laws
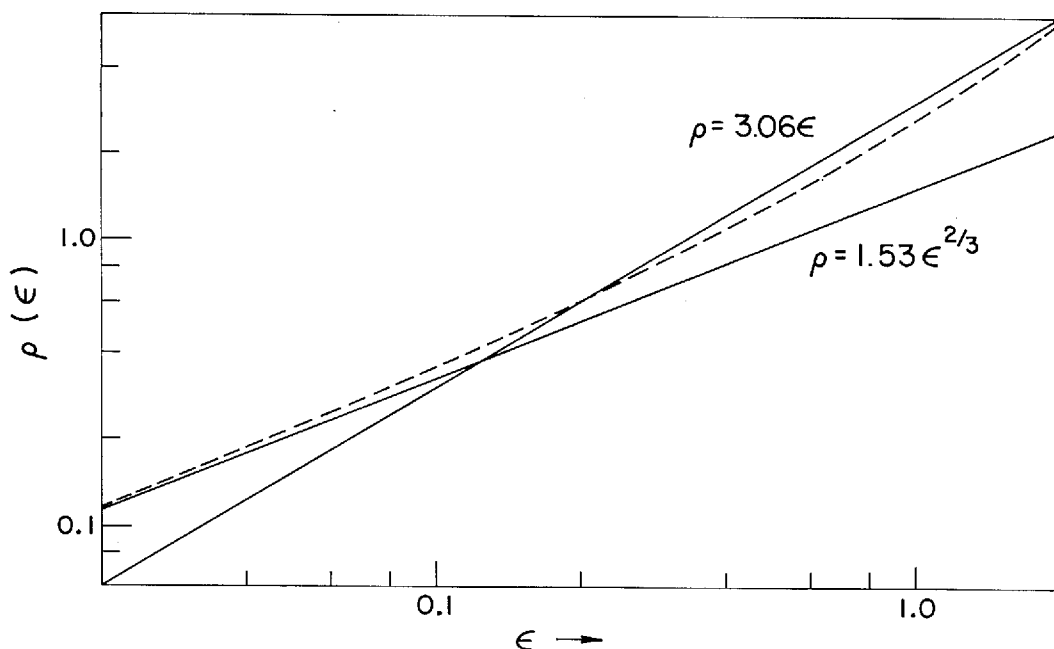
Fig. 3. Reduced Path Lengths. Dashed line: Integrated from eq. (3). Thin solid lines: eq. (11).

$$s(\varepsilon) \;=\; \frac{\lambda_m}{2(1-m)}\varepsilon^{1-2m} \tag{10}$$

corresponding to

$$S(E) \;=\; \frac{C}{1-m}\,\gamma^{1-m}E^{1-2m}. \tag{10a}$$

Fig. 3 compares the path length following from eq. (3) with the power law path lengths

$$\varrho(\varepsilon) \;=\; \frac{(1-m)}{m\cdot\lambda_m}\varepsilon^{2m}. \tag{11}$$

If $\sim 20\,\%$ accuracy in both stopping and path length is required for the power cross-sections to be acceptable we obtain the following ranges of validity:

$$\left. \begin{array}{ll} m \,=\, 1/3 & \text{for}\quad \varepsilon \lesssim 0.2 \\[4pt] m \,=\, 1/2 & \text{for}\quad 0.08 \lesssim \varepsilon \lesssim 2. \end{array} \right\} \tag{12}$$

Note also that the power law stopping with $m \,=\, 1/3$ is indistinguishable from the Lindhard stopping on the scale of the figure for $\varepsilon \lesssim 0.02$, while the path length figure indicates that the $m \,=\, 1/2$ stopping cross-section is a reasonable overall approximation. (Bohr 1948; Nielsen, 1956). At very low energies all these cross

sections should be taken with caution since the Thomas-Fermi treatment becomes questionable.

It may be noted that in a previous communication (SIGMUND & SANDERS, 1967) we used a slightly different coefficient in the power cross section for $m = 1/3$ ($\lambda_{1/3} = 1.19$), and energy limits that differed from eq. (12). This is because both were determined only from the range-energy relationship.

Electronic Energy Loss

According to LINDHARD & SCHARFF (1961) electronic stopping can be approximated by

$$\left(\frac{d\varepsilon}{d\varrho}\right)_e = -k\varepsilon^{1/2} \quad \text{for} \quad E \lesssim Z_1^{4/3} A_1 \cdot 25\,\text{keV}, \tag{13}$$

where k is of the order of 0.1 to 0.2 except for $Z_1 \langle\langle Z_2$ where k can become larger than 1. A_1 is the atomic weight of the ion. Thus, for $\varepsilon \lesssim 1$ electronic stopping is usually a minor correction, unless $Z_1 \lesssim 10\, Z_2$, when it may not be neglected (SCHIØTT, 1966).

Deposited Energy: Simple Estimate

LINDHARD et al. (1963 b) established their basic range vs. energy relationship by evaluating the integral of eq. (9). This would be appropriate for continuous slowing down along a straight line. Subsequently they showed that (9) is a good approximation to the total travelled path length even when the slowing down is not continuous, and that the path length does not deviate much from the projected range as long as $M_1 > M_2$. It is tempting to make a similar estimate for the deposited energy. For purely elastic stopping the amount of energy deposited in *primary collisions* on the path element dx is given by

$$dE = N\,S(E(x))\,dx = F(x)\,dx \tag{14}$$

where x is the path length travelled from the initial energy E down to energy $E(x)$. Eq. (14) defines a depth distribution function $F(x)$ of energy loss, which neglects the fact that energy is carried away by recoiling atoms.

For the case of the power cross section, equation (5), we obtain, by inserting (10 a) into (7),

$$R(E) = \frac{(1-m)}{2m}\frac{\gamma^{m-1}}{NC}E^{2m} \tag{15}$$

and, from (10 a) and (14),

$$F(x) = \frac{E}{2mR}(1 - x/R)^{\frac{1}{2m}-1} \quad \text{for} \quad 0 \le x \le R$$

$$0 \qquad\qquad\qquad\qquad \text{otherwise.}$$

(16)

It is easily verified from (16) that

$$\int_{-\infty}^{\infty} F(x)dx = E;$$

(17)

$$\langle x \rangle = \frac{1}{E}\int_{-\infty}^{\infty} x F(x)dx = \frac{2m}{1+2m}R;$$

(18)

$$\frac{\langle \Delta x^2 \rangle}{\langle x \rangle^2} = \frac{\langle x^2 \rangle - \langle x \rangle^2}{\langle x \rangle^2} = \frac{1}{1+4m}.$$

(19)

Eq. (17) states that the total amount of energy deposited along the whole trajectory is just the initially available kinetic energy, and (18, 19) determine the center and the width of the distribution. The path length $R(E)$ is an appropriate length unit to eliminate the explicit dependence on energy.

In fact, it will be seen in the following that, provided a number of simplifying assumptions can be made, the path length $R(E)$ as given by eq. (15) is a length unit that determines the energy dependence of the extension of the collision cascade in all three dimensions. Hence, within the limit of the power cross section the shape of the cascade can be considered independent of energy. This is one of the simplifying features of the power cross section.

The two major simplifications leading to eqs. (18) and (19) are the assumption of motion along a straight line, which breaks down for $M_1 \lesssim M_2$, and the neglect of energy transported a measurable distance away from the particle trajectory by energetic recoil atoms. Since the latter assumption becomes questionable for $M_1 \gtrsim M_2$ we have to conclude that (14) is probably less useful than eq. (7).

Estimates of the type discussed in this paragraph are more successful at high ion energies when the slowing down of the ion is governed by electronic stopping. Then, the ion trajectory becomes straightened out even for $M_1 \ll M_2$, and the recoil ranges tend to become relatively small as compared to ion ranges unless $M_1 \gg M_2$. Obviously, eq. (17) is no longer valid then. An estimate of this type has been made previously (SIGMUND & SAN-

DERS, 1967). BRICE (1970) improved the procedure by taking into account energy loss straggling and path length correction as well as electronic energy loss by recoil atoms. BRICE's approach is feasible if none of the three corrections has a dominating effect on the distribution. The finite range of recoiling atoms was neglected.*

3. Basic Integral Equations

It is well known that the distribution of ion ranges in a random medium is determined by an integro-differential equation of the transport type. The same is true for the distribution of deposited energy. There is, however, a major difference between the two distributions. For any *single* ion path the range distribution shrinks to one point, namely the end point of the ion's trajectory. The distribution is then *generated* by repeating the slowing-down process a sufficiently large number of times with the same initial conditions. For any single ion path however, the distribution of deposited energy extends over a region whose dimensions are expected to be of the order of the ion range. If we repeat the slowing down process many times with the same initial conditions, these distributions will be *superimposed* to create a distribution that, in general, extends over a larger region in space. Hence, while the range distribution contains all information that can possibly be obtained about the *end points* of the ion trajectories for random slowing down, the spatial distribution of deposited energy will in general *not* contain all *possible* information about the *location of energy* at the end of the slowing-down process: for example, one could also inquire about the energy distribution given the projectile's path, or end point. Whether the information contained in the distribution function of deposited energy is sufficient depends on the specific experimental situation. If it is not, one has to consider correlation functions. These will be investigated in another paper.

Average Deposited Energy

We first consider a monatomic, random, and infinite medium characterized by an atomic number Z_2, atomic mass M_2, density of atoms N; and a projectile of the same type (Z_2, M_2) starting its motion at a point $\vec{r} = 0$ with a velocity $\vec{v}$. Only binary collisions are considered. The energy or damage distribution function, $F(\vec{r}, \vec{v})$, is defined so that $F(\vec{r}, \vec{v}) d^3r$ is the

*Note added in proof: Comparison with recent results of P. SIGMUND, M. T. MATTHIES, and D. L. PHILLIPS (to be publ.) shows that for equal masses of target and projectile, Brice's approach is valid for $\varepsilon \gg 1$.

average amount of energy located in the volume element $(\vec{r}, d^3r)$, after both the projectile and all recoiling atoms have slowed down below a certain energy limit that is very small compared to the initial energy. In most numerical calculations in this paper we take this limiting energy to be zero; we discuss this assumption in a subsequent paragraph. It is implied that the time after which the location of energy is determined is long enough to ensure that energy no longer propagates any appreciable distance via *collision* processes, but short enough to prevent sound waves from carrying the energy away. (The time constant for slowing-down is of the order of 10^{-13} seconds for keV ions, i.e. of the order of only one lattice vibrational period).

For the moment we neglect the binding forces acting on target atoms. Then, from the definition and energy conservation it follows that

$$\int F(\vec{r}, \vec{v}) d^3r = E. \tag{20}$$

$F(\vec{r}, \vec{v})$ satisfies the integral equation

$$-\frac{\vec{v}}{v}\frac{\partial}{\partial \vec{r}} F(\vec{r}, \vec{v}) = N\int d\sigma [F(\vec{r}, \vec{v}) - F(\vec{r}, \vec{v}') - F(\vec{r}, \vec{v}'')], \tag{21}$$

where

$$\left.\begin{array}{l} v = |\vec{v}| ; \\ \vec{v}' = \text{velocity of scattered particle}; \\ \vec{v}'' = \text{velocity of recoiling atom}; \\ d\sigma = \text{differential cross section} = K(\vec{v}, \vec{v}', \vec{v}'') d^3\vec{v}' d^3\vec{v}'' ; \end{array}\right\} \tag{21 a}$$

(21) is analogous to the integral equation for the vector range (SANDERS 1968a) and is also derived in the same way. The argument follows that of LINDHARD et al. (1963a, b), and, briefly, is this. The distribution F is that due to a particle starting at the origin with velocity $\vec{v}$. After this original particle has moved a short vector distance $\vec{\delta R}$ there is one particle at $\vec{\delta R}$ with velocity $\vec{v}$, if no scattering has taken place, or, if a collision has taken place, with probability $N|\vec{\delta R}|d\sigma$, two moving particles, with velocities $\vec{v}'$ and $\vec{v}''$. The original distribution must be the same as the superposition of distributions with these new initial conditions. Thus, to first order in $\vec{\delta R}$, and using the translational invariance of the medium,

$$F(\vec{r}, \vec{v}) = N|\vec{\delta R}|\int d\sigma [F(\vec{r}, \vec{v}') + F(\vec{r}, \vec{v}'')] + (1 - N|\vec{\delta R}|\int d\sigma) F(\vec{r} - \vec{\delta R}, \vec{v}) \tag{22}$$

where the integrations are over all possible (binary) collisions. Expanding the second term on the right to first order in $\vec{\delta R}$, and using $\vec{\delta R}/|\vec{\delta R}| = \vec{v}/v$, we obtain eq. (21).

We now proceed to the case of a monatomic medium, characterized by Z_2, M_2, N, and bombarded by a projectile with atomic number Z_1 and mass M_1. We have to distinguish between the function $F(\vec{r},\vec{v})$ defined as before (i.e., for a bombarding *target* atom) and a new function $F_{(1)}(\vec{r},\vec{v})$ that determines the spatial distribution of energy as a consequence of the projectile ion (Z_1,M_1) slowing down from velocity $\vec{v}$. Collisions between the ion and target atoms are described by a cross section $d\sigma_{(1)}$, while $d\sigma$ still describes collisions between target atoms. By the same argument as previously we obtain

$$\int F_{(1)}(\vec{r},\vec{v})d^3r = E; \tag{23}$$

and

$$-\frac{\vec{v}}{v}\frac{\partial}{\partial \vec{r}}F_{(1)}(\vec{r},\vec{v}) = N\int d\sigma_{(1)}[F_{(1)}(\vec{r},\vec{v}) - F_{(1)}(\vec{r},\vec{v}\,') - F(\vec{r},\vec{v}\,'')]. \tag{24}$$

The essential difference between (21) and (24) is that the former is homogeneous while the latter contains $F(\vec{r},\vec{v}\,'')$ as an inhomogeneity. This is a major complication of the computational work as compared to the range distribution $F_{(R)}(\vec{r},\vec{v})$ where we have (SANDERS, 1968 a)

$$\int F_{(R)}(\vec{r},\vec{v})d^3r = 1 \tag{25}$$

$$-\frac{\vec{v}}{v}\frac{\partial}{\partial \vec{r}}F_{(R)}(\vec{r},\vec{v}) = N\int d\sigma_{(1)}[F_{(R)}(\vec{r},\vec{v}) - F_{(R)}(\vec{r},\vec{v}\,')] \tag{26}$$

for either equal or unequal masses.

Next, we consider the case of a polyatomic medium containing atoms of type j (Z_j,M_j), $(j = 2,3,4..)$, where collisions between atoms i (striking) and j (struck) are described by a cross section $d\sigma_{(ij)}$. We define $F_{(ij)}(\vec{r},\vec{v})d^3r$ as the average amount of energy located in the volume element d^3r as kinetic energy of atoms of type j, as a consequence of an atom of type i slowing down from a point $\vec{r} = 0$ with initial velocity $\vec{v}$. By generalizing the previous argument we obtain

$$\sum_j \int F_{(ij)}(\vec{r},\vec{v})d^3r = E; \tag{27}$$

and

$$-\frac{\vec{v}}{v}\frac{\partial}{\partial \vec{r}}F_{(ij)}(\vec{r},\vec{v}) = \sum_k N_k \int d\sigma_{(ik)}[F_{(ij)}(\vec{r},\vec{v}) - F_{(ij)}(\vec{r},\vec{v}') - F_{(kj)}(\vec{r},\vec{v}'')]. \quad (28)$$

Eqs. (27) and (28) are in general not sufficient to determine $F_{(ij)}(\vec{r},\vec{v})$ uniquely. Also, the sharing of energy between the various components of the system may lead to conceptual difficulties, especially in solids. In many practical problems $F_{(ij)}(\vec{r},\vec{v})$ may not even be of interest. One may need only the simpler energy distribution functions

$$F_{(i)}(\vec{r},\vec{v}) = \sum_j F_{(ij)}(\vec{r},\vec{v})$$

that determine the location of energy irrespective of its distribution among the constituent atoms. These satisfy the following equations:

$$\int F_{(i)}(\vec{r},\vec{v})d^3r = E \qquad\qquad (27\,a)$$

and

$$-\frac{\vec{v}}{v}\frac{\partial}{\partial \vec{r}}F_{(i)}(\vec{r},\vec{v}) = \sum_k N_k \int d\sigma_{(ik)}[F_{(i)}(\vec{r},\vec{v}) - F_{(i)}(\vec{r},\vec{v}') - F_{(k)}(\vec{r},\vec{v}'')] \quad (28\,a)$$

which follow immediately from (27) and (28). Eq. (28 a) represents a system of as many coupled integro-differential equations as there are components in the system. Once all $F_{(i)}(\vec{r},\vec{v})$ have been determined—which may be a cumbersome procedure—it is relatively easy to determine the function $F_{(1)}$ determining the deposited energy in a poly-atomic medium bombarded by an ion (Z_1, M_1) that is different from any of its components. We obtain

$$\int F_{(1)}(\vec{r},\vec{v})d^3r = E, \qquad\qquad (27\,b)$$

$$-\frac{\vec{v}}{v}\frac{\partial}{\partial \vec{r}}F_{(1)}(\vec{r},\vec{v}) = \sum_k N_k \int d\sigma_{(1k)}[F_{(1)}(\vec{r},\vec{v}) - F_{(1)}(\vec{r},\vec{v}') - F_{(k)}(\vec{r},\vec{v}'')], \quad (28\,b)$$

i. e. only one additional equation containing all $F_{(k)}$ as inhomogeneities.

The corresponding equations for the ion range are

$$\int F_{(R)}(\vec{r},\vec{v})d^3r = 1, \qquad\qquad (25\,a)$$

$$-\frac{\vec{v}}{v}\frac{\partial}{\partial \vec{r}}F_{(R)}(\vec{r},\vec{v}) = \sum_k N_k \int d\sigma_{(1k)}[F_{(R)}(\vec{r},\vec{v}) - F_{(R)}(\vec{r},\vec{v}')]. \qquad (26\,a)$$

Special cases of (26 a) have been considered by SANDERS (1968 a), SCHIØTT (1968), and BAROODY (1969).

A number of other authors have used integral equations of this type to investigate ion ranges (HOLMES & LEIBFRIED, 1960; LEIBFRIED, 1962, 1963; BAROODY, 1964, 1965; LEIBFRIED & MIKA, 1965) and damage distributions (CORCIOVEI et al., 1962, 1963, 1966; v. JAN., 1964; DEDERICHS, 1965; DEDERICHS et al., 1966). All the work on damage distributions and part of the range work dealt only with the equal mass case. Furthermore, all of these investigations except the one by BAROODY (1965) used hard-sphere or hard-sphere-like scattering in the numerical work. We have shown in an earlier communication (SIGMUND & SANDERS, 1967) that hard-sphere scattering is too poor an approximation to allow quantitative conclusions, and sometimes even produces results that differ qualitatively from those obtained with the (more accurate) power cross sections.

Finally we mention that the integral equations derived in this paragraph are rather general and apply also to situations other than heavy ions slowing down by elastic collisions. As long as the cross sections are not specified the equations apply as well to moving electrons, neutrons, etc., and the different components of the system in (28) may also be electrons on the one side and atoms on the other. In this case, of course, the conventional picture of a series of successive two-particle collisions is not necessarily applicable. For example, from one impact of an ion on an atom there may arise several energetic electrons. In such a case the recoil term $F(\vec{r}, \vec{v}'')$ in (24) or any equivalent equation has to be replaced by $\sum_{\nu} F_{(\nu)}(\vec{r}, \vec{v}_\nu'')$

which is the sum of the contributions to $F(\vec{r}, \vec{v})$ of all particles originating from a collision (LINDHARD et al., 1963 a, b). These more general cases will be dealt with in a later paper.

Deposited Energy: Relation to Damage Effects

In the foregoing paragraph we assumed that the process of dissipation of kinetic energy can continue to arbitrarily low particle energies, via binary collisions between freely moving atoms. Obviously, at low particle energies the effects of atomic binding have to be considered. We limit our discussion to a solid target, which may be amorphous or crystalline, the effects of regular lattice structure on slowing down being neglected. Two effects of potential energy appear to be dominant.

a) There will be a certain minimum energy W for a particle either to get displaced "permanently" from its original position or to displace other

atoms. This has the immediate consequence that the quantity E^{2m}/NC is no longer a universal length unit, since e.g. W^{2m}/NC also has the dimension of a length. W may be a function of the position of the atom and its direction of motion. In the bulk, W is the order of the radiation damage threshold energy E_d ($\sim 10 - 100$ eV), while considerably smaller values of W are expected at and near the surface. The energy lost in subthreshold collisions ($T < W$) will normally be converted into heat and thus not be of interest to radiation damage (except that subthreshold collisions may cause annealing of existing radiation damage). From the theory of displacement cascades it is well known that the number $N(E)$ of permanently displaced atoms is of the order of $N(E) \approx E/2W$ for $E \gg W$, W now being a suitable average threshold energy (LEHMANN, 1961, SIGMUND, 1969 b, c). Thus, one would expect that, in the average, one atom will be displaced for each volume element containing an amount of $\sim 2W$ of deposited energy. Provided that the initial energy $E \gg 2W$, this volume element is much smaller than the total extension of the collision cascade. Hence, in the limit of $E \gg W$, the introduction of a finite threshold energy W should not affect the gross spatial distribution of deposited energy. This will be formulated more quantitatively in sect. 5. The close similarity to the spatial distribution of interstitials or vacancies can be formulated more quantitatively, too, if certain additional assumptions are made concerning the displacement process (DEDERICHS, 1965; v. JAN, 1964; SIGMUND et al., 1968).

b) Upon leaving its rest position, an atom will in general lose an amount of energy U that may depend on position, energy, and direction of motion of the atom. U may be of the order of the cohesive energy or less. Also, the lattice may be left in an excited state, so that some of the lattice potential energy is converted into kinetic energy of the atoms surrounding the initial position of the displaced atom. Although one could in principle define the deposited energy function $F(\vec{r},\vec{v})$ in such a way that energy is conserved, so eq. (20) holds, it is more convenient not to include the above amounts of potential energy in the energy balance. Then, of course, eq. (20) does not hold. The energy defect can be found by counting the number of recoil events in which potential energy is converted. For example, let us assume a sharp threshold energy W as defined above, and let a particle stop dissipating energy as soon as its energy is below W. Let us further assume that a recoiling atom loses a fixed amount of energy U upon leaving its initial position. Then, the total number of atoms that recoil with an energy in the interval (E_0, dE_0) in a collision cascade initiated by an atom of energy E is given by (SIGMUND, 1969 c).

$$F(E, E_0)dE_0 = \frac{m}{\psi(1) - \psi(1 - m)} \frac{E}{(E_0 + U)^{1-m} E_0^{1+m}} dE_0, \qquad (29)$$

for $E \gg E_0 \gg U$ assuming the scattering to be described by the power cross section eq. (5). The function $\psi(x) = (d/dx) \ln \Gamma(x)$ is the digamma function.

The total amount of kinetic energy lost during slowing down to W is then given by

$$\Delta E = U \cdot \int_W^E F(E, E_0)dE_0 = \frac{(1 + U/W)^m - 1}{\psi(1) - \psi(1 - m)} E. \qquad (29a)$$

Depending on the ratio of U/W, ΔE can be a sizable fraction of E. If U/W is small, the fraction $\Delta E/E$ is of the order of U/W. However, even though this energy defect may not be negligible when the *amount* of deposited energy is considered, the *spatial distribution* is hardly affected at all, since eq. (29) clearly shows that the great majority of these energy quanta U are lost by atoms recoiling with very low energy E_0, i.e. that do not affect the spatial distribution. In fact, for $E_0 \gg U$ we have an $\sim E_0^{-2}$ recoil density. This point also will be elucidated more quantitatively in sect. 5.

Apart from the effects of potential energy, another limit is imposed on the energy dissipation when essentially every atom within the cascade volume is set in motion with a sizable energy. This defines a limiting energy E^* of the order of $\sim E/N\Omega$, where Ω is the volume covered by the cascade. Rough estimates indicate that E^* is usually small compared with W, so this effect will be assumed negligible in the following.*

The above discussion concentrated on the spatial distribution of *displaced* atoms, as characterized by a threshold energy W. Obviously, the argument also applies to the spatial distribution of recoils with energies different from W, for example, those described by the recoil density $F(E, E_0)$ of eq. (29), and to the slowing-down-density that dominates the numbers of atoms *moving* in a certain energy interval under steady-state conditions. The latter quantity is of great use in sputtering theory (SIGMUND, 1969a). In fact, the number of atoms moving with an energy greater than the sputtering threshold energy is proportional to the total energy, but the fraction of those that are close enough to the target surface to be sputtered is determined by the energy deposition function. Also the spatial distribution of the *collision density* can be reduced to the deposited energy distribution, provided that

---

*Note added in proof: E^* can become comparable to W for very heavy ions in the lower keV region. Presumably, this affects the number of atoms set in motion (recoil density) but hardly the spatial distribution.

the collision density is defined to count all collision products in suitable energy intervals (SANDERS, 1966, 1968b; ROBINSON, 1965b; KOSTIN, 1965; FELDER & KOSTIN, 1966). Various concepts of collision density have been introduced in the literature; a discussion of their physical significance is a delicate task, but not the subject of this paper.

Finally, we mention that the assumption of complete randomness of the system under consideration is not necessarily applicable to crystalline targets. The assumption is not valid when single crystals are bombarded under channelling conditions, and even in polycrystals, or single crystals bombarded in a "random" direction, there is a possibility for scattering of ions and recoil atoms into a channel, and of linear collision chains travelling over a distance exceeding that for random slowing down at the same energy. It is implied that random-slowing-down theory holds approximately only when these lattice effects are rare, or when the corresponding ranges are small compared with the total extension of the collision cascade. Obviously, the significance of these lattice effects depends on the target, damage state, ion dose, and irradiation temperature.

Probability Distribution of Deposited Energy

It was mentioned earlier that the distribution function $F(\vec{r},\vec{v})$ and related quantities do not contain all possible information on the distribution of deposited energy. At present we go only one step further and derive an equation for the probability distribution of deposited energy, of which $F(\vec{r},\vec{v})$ is the average. We define the function $G(\vec{r},\vec{v},P)$ in the following way.

$G(\vec{r},\vec{v},P)\ dP$ is the probability that an amount of energy between Pd^3r and $(P+dP)d^3r$ is deposited in the volume element $(\vec{r},d^3r)$, by a projectile starting with velocity $\vec{v}$ at $\vec{r} = 0$, and all generations of recoiling particles.

Obviously G has to be normalized:

$$\int_0^\infty G(\vec{r},\vec{v},P)dP = 1. \qquad (30)$$

The average energy deposited in $(\vec{r},d^3r)$ is then

$$\int_{P=0}^\infty (Pd^3r)G(\vec{r},\vec{v},P)dP = F(\vec{r},\vec{v})d^3r,$$

so

$$F(\vec{r},\vec{v}) = \int_0^\infty PG(\vec{r},\vec{v},P)dP \qquad (31)$$

where $F(\vec{r},\vec{v})$ is the function defined by (20) and (21) with W finite or zero.

By use of the argument leading to (22) we obtain the following equation for $G(\vec{r},\vec{v},P)$:

$$G(\vec{r},\vec{v},P) = N|\vec{\delta R}| \int d\sigma \int_0^P dQ G(\vec{r},\vec{v}',Q)G(\vec{r},\vec{v}'',P-Q)$$

$$+ (1 - N|\vec{\delta R}| \int d\sigma)G(\vec{r}-\vec{\delta R},\vec{v},P). \tag{32}$$

The first term on the right side expresses the fact that the total energy deposited in $(\vec{r},d^3r)$ by the scattered projectile and the recoiling particle must sum to P. Letting δR go to zero we obtain

$$-\frac{\vec{v}}{v}\frac{\partial}{\partial \vec{r}}G(\vec{r},\vec{v},P) = N \int d\sigma \left[G(\vec{r},\vec{v},P) - \int_0^P dQ G(\vec{r},\vec{v}',Q)G(\vec{r},\vec{v}'',P-Q) \right]. \tag{33}$$

We want to derive eq. (21) from (33). Multiplying (33) by P and integrating over P we obtain, by use of (31)

$$-\frac{\vec{v}}{v}\frac{\partial}{\partial \vec{r}}F(\vec{r},\vec{v}) = N \int d\sigma \left[F(\vec{r},\vec{v}) - \int_0^\infty dP \int_0^P dQ \cdot P G(\vec{r},\vec{v}',Q)G(\vec{r},\vec{v}'',P-Q) \right]. \tag{34}$$

Substituting $P \to P + Q$ in the second term on the right side in (34) we obtain

$$-\int_0^\infty dP \int_0^\infty dQ(P+Q)G(\vec{r},\vec{v}',Q)G(\vec{r},\vec{v}'',P) = -F(\vec{r},\vec{v}') - F(\vec{r},\vec{v}''), \tag{35}$$

using (30) and (31). Inserting (35) into (34) we arrive at (21).

Eq. (33) could easily be generalized to all the cases discussed at the beginning of this section. This is merely a matter of notation.

4. Equations for Spatial Averages

There are several methods available to find approximate solutions of integral equations of the type derived in the preceding section. These are reviewed in textbooks and review articles on slowing down of neutrons, penetration of X-rays, etc. But even in the highly simplified case of hard-sphere scattering it has not been possible to find the exact solutions. It is, however, possible to calculate exact expressions for *averages* over the distribution functions, for a certain class of cross sections including the power cross sections specified in (5). We shall, therefore, calculate averages first, in order to have a solid basis for comparison with experiments, and try to construct distribution functions from the averages, rather than attack directly the equations for the distribution functions. The derivations in the present section are based on standard methods developed several decades

ago in other penetration problems and used also in the theory of ion ranges. We sketch the derivations for completeness and because of some slight differences from the equations occurring in other problems.

Plane Monodirectional Source

In experiments with ion beams one has a more or less monodirectional source of projectiles, hitting a target with a more or less planar surface. It is convenient to solve the integral equations for planar geometry. This determines the depth distribution of the deposited energy.

Let us assume a coordinate system with the x-axis perpendicular to the surface of the target, and a plane monodirectional source at $x = 0$. Then $F(\vec{r},\vec{v})$ does not depend on y and z so (20) and (21) read

$$\int_{-\infty}^{\infty} F(x,\vec{v})\,dx = E, \tag{36}$$

$$-\cos\theta\,\frac{\partial}{\partial x}F(x,\vec{v}) = N\int d\sigma[F(x,\vec{v}) - F(x,\vec{v}') - F(x,\vec{v}'')], \tag{37}$$

where $F(x,\vec{v})dx = dx\int F(\vec{r},\vec{v})dydz$ is the energy deposited in the layer (x,dx) on the average by *one* projectile starting in the plane $x = 0$ with velocity $\vec{v}$, and $\cos\theta = \eta$ is the directional cosine of $\vec{v}$ with respect to the x-axis. Note that (37) still requires the medium to be infinite, and that the "surface" at $x = 0$ is only a reference plane. Whether our results apply to a target with a real surface depends on the importance of scattering back and forth through the plane $x = 0$.

For an isotropic medium, $F(x,\vec{v})$ cannot depend on the azimuth of $\vec{v}$ with respect to the x-axis. Hence

$$F(x,\vec{v}) \equiv F(x,E,\eta) = \sum_{l=0}^{\infty} (2l + 1)F_l(x,E)P_l(\eta), \tag{38}$$

after changing from velocity to energy variables, and expanding F in terms of Legendre polynomials. The factor $(2l + 1)$ is included for convenience. The coefficients $F_l(x,E)$ are then given by

$$F_l(x,E) = \frac{1}{2}\int_{-1}^{1} d\eta F(x,E,\eta)P_l(\eta) \tag{38 a}$$

Integrating (38 a) over x, and taking into account eq. (36), we obtain

$$\int\limits_{-\infty}^{\infty} dx F_l(x, E) = \delta_{l0} E. \tag{39}$$

Eq. (37) will now be reduced to a set of equations for the $F_l(x,E)$. On the left side we employ the recurrence formula for Legendre polynomials, so that

$$\left. \begin{aligned} - \eta \frac{\partial}{\partial x} F(x, \vec{v}) &= - \sum_l \frac{\partial}{\partial x} F_l(x, E) \cdot [(l+1) P_{l+1}(\eta) + l P_{l-1}(\eta)] \\ &= - \sum_l \left[l \frac{\partial}{\partial x} F_{l-1}(x, E) + (l+1) \frac{\partial}{\partial x} F_{l+1}(x, E) \right] P_l(\eta). \end{aligned} \right\} \tag{40 a}$$

The first integral on the right of (37) is given by

$$N \int d\sigma F(x, \vec{v}) = \sum_l (2l + 1) N \int d\sigma(E, T) F_l(x, E) P_l(\eta), \tag{40 b}$$

while the second,

$$- N \int d\sigma F(x, \vec{v}') = - \sum_l (2l + 1) N \int d\sigma(\vec{v}, \vec{v}') F_l(x, E - T) P_l(\eta'),$$

has to be transformed in such a way that η, not η', is the variable in $P_l(\eta)$. η' is the directional cosine of $\vec{v}'$ with respect to the x-axis. We can express the cross section for elastic collisions by

$$d\sigma(\vec{v}, \vec{v}') = d\sigma(E, T) \frac{d\vec{e}'}{2\pi} \delta(\vec{e} \cdot \vec{e}' - \cos \varphi'), \tag{41}$$

where $\vec{e} = \vec{v}/v$, $\vec{e}' = \vec{v}'/v'$ and φ' is the laboratory scattering angle of the projectile, a function of E and T. We expand the δ-function,

$$\delta(\vec{e} \cdot \vec{e}' - \cos \varphi') = \sum_{l=0}^{\infty} \frac{2l+1}{2} P_l(\vec{e} \cdot \vec{e}') P_l(\cos \varphi'),$$

and insert the addition theorem for spherical harmonics,

$$P_l(\vec{e} \cdot \vec{e}') = \sum_{\mu=-l}^{l} \frac{4\pi}{2l+1} Y_{l\mu}(\vec{e}) Y_{l\mu}^*(\vec{e}'),$$

where $Y_{l\mu}(\vec{e})$ are spherical harmonics in the notation of SCHIFF (1955). With the x-axis as a reference axis, the integral over $\vec{e}'$ can be performed and yields

$$- N \int d\sigma F(x,\vec{v}') = -\sum_l (2l+1) N \int d\sigma(E,T) P_l(\cos\varphi') F_l(x, E-T) P_l(\eta). \quad (40\,\text{c})$$

A similar calculation for the third integral in (37) yields

$$- N \int d\sigma F(x,\vec{v}'') = -\sum_l (2l+1) N \int d\sigma(E,T) P_l(\cos\varphi'') F_l(x,T) P_l(\eta), \quad (40\,\text{d})$$

where φ'' is the laboratory scattering angle of the recoiling atom. Collecting equations (40 a–d) we obtain

$$\left. \begin{aligned} -l \frac{\partial}{\partial x} F_{l-1}(x,E) - (l+1)\frac{\partial}{\partial x} F_{l+1}(x,E) &= (2l+1) N \int d\sigma(E,T) \\ \cdot [F_l(x,E) - P_l(\cos\varphi') F_l(x, E-T) &- P_l(\cos\varphi'') F_l(x,T)]. \end{aligned} \right\} \quad (42)$$

Spatial averages over the distribution function $F(x,\vec{v})$ are obtained by integration of (38),

$$\int_{-\infty}^{\infty} x^n dx F(x,\vec{v}) = \sum_{l=0}^{\infty} (2l+1) F_l{}^n(E) P_l(\eta), \quad (43)$$

where

$$F_l{}^n(E) = \int_{-\infty}^{\infty} dx\, x^n F_l(x,E). \quad (43\,\text{a})$$

So, by integrating (42),

$$\left. \begin{aligned} n l F_{l-1}^{n-1}(E) + n(l+1) F_{l+1}^{n-1}(E) &= (2l+1) N \int d\sigma \\ \cdot [F_l{}^n(E) - P_l(\cos\varphi') F_l{}^n(E-T) &- P_l(\cos\varphi'') F_l{}^n(T)]. \end{aligned} \right\} \quad (44)$$

Using the notation of (43 a), (39) reads

$$F_l{}^0(E) = \delta_{l0} E. \quad (45)$$

Thus (44) represents a system of integral equations that can be solved stepwise with increasing n, the case $n = 1$ being defined by (45). Obviously, for $n = 1$ only the moment $F_1^1(E)$ is different from zero since, because of eq. (45), eq. (44) is homogeneous for $n = 1$ and $l \neq 1$. Similar arguments

apply to higher order moments. It turns out that $F_l^n \neq 0$ only for $l \leq n$ and $l + n$ even. Thus, the sum (43) is always finite.

Eq. (44) has been derived from (21) for the simplest of the distribution functions discussed in the previous section. Generalization to other functions is a matter only of adding the right indices. For example, (23) reduces to

$$
\left.
\begin{aligned}
& nl F_{(1)\,l-1}^{\,n-1}(E) + n(l+1) F_{(1)\,l+1}^{\,n-1}(E) = (2l+1) N \int d\sigma_{(1)} \\
& \quad \cdot [F_{(1)\,l}^{\,n}(E) - P_l(\cos\varphi'_{(1)}) F_{(1)\,l}^{\,n}(E-T) \\
& \quad - P_l(\cos\varphi''_{(1)}) F_l^{\,n}(T)],
\end{aligned}
\right\} \quad (46)
$$

where $\varphi'_{(1)}$ and $\varphi''_{(1)}$ are laboratory scattering angles for $M_1 \neq M_2$, and $F_{(1)\,l}^{\,n}(E)$ derives from $F_{(1)}(\vec{r},\vec{v})$ in the same way as $F_l^n(E)$ from $F(\vec{r},\vec{v})$. Furthermore, from (22) and (45),

$$
F_{(1)\,l}^{\,0}(E) = \delta_{l0} E. \tag{47}
$$

If the last term on the right side of (46) is omitted one obtains the equation for the moments of the projected range distribution. Eq. (47) has then to be replaced by $F_{(1)\,l}^{\,0}(E) = \delta_{l0}$. This system of equations has been studied by BAROODY (1964, 1965).

Point Monodirectional Source

If one is interested in the extension in three dimensions of collision cascades it may be more convenient to consider a point source. This case has been studied by CORCIOVEI et al. (1962, 1963, 1966), v. JAN (1964), DEDERICHS (1965), and SANDERS (1968), as well as in our previous communication (SIGMUND & SANDERS, 1967), and in all the range work quoted previously, with the exception of BAROODY (1964, 1965, 1969). A general relation between the solutions for plane and point sources has been derived by BERGER & SPENCER (1959), and is quoted in Appendix C. We remind the reader that $F(\vec{r},\vec{v})$ does not in general determine the dimensions of a single cascade but those of the region covered by a great number of cascades with the same initial conditions.

With a point source at $\vec{r} = 0$, the initial velocity vector $\vec{v}$ is used as a reference axis X. The Y and Z axes are perpendicular to $\vec{v}$.

We expand

$$
F(\vec{r},\vec{v}) \equiv \sum_l (2l+1) f_l(r,E) P_l(\zeta), \tag{48}
$$

where $\zeta = (\vec{r}\cdot\vec{v})/(rv)$. For the moments

$$f_l^n(E) = 4\pi \int_0^\infty r^{2+n} dr\, f_l(r,E) \tag{49}$$

we obtain the following set of equations:

$$
\left.
\begin{aligned}
&l(l+n+1)f_{l-1}^{n-1}(E) + (l+1)(n-l)f_{l+1}^{n-1}(E) = (2l+1)N\int d\sigma \\
&[f_l^n(E) - P_l(\cos\varphi')f_l^n(E-T) - P_l(\cos\varphi'')f_l^n(T)],
\end{aligned}
\right\} \tag{50}
$$

and the normalization condition

$$f_0^0(E) = E. \tag{51}$$

The $f_l^0(E)$, $l \neq 0$ are not prescribed, in contrast to (45). However, those moments $f_l^n(E)$ that can be calculated recursively from $f_0^0(E)$ determine the spatial averages $\int X^i Y^j Z^k F(\vec{r},\vec{v})d^3r$ for integer $i,j,k \geq 0$. From (48) we obtain

$$
\left.
\begin{aligned}
\int X^i Y^j Z^k F(\vec{r},\vec{v})d^3r = &\sum_l (2l+1)f_l^{i+j+k}(E)\frac{1}{2}\int_{-1}^1 d\zeta\,\zeta^i(1-\zeta^2)^{\frac{j+k}{2}}P_l(\zeta) \\
&\times \frac{1}{2\pi}\int_0^{2\pi} d\chi \cos^j\chi \sin^k\chi
\end{aligned}
\right\} \tag{52}
$$

which can be readily evaluated. The resulting general expression looks more complicated than it is so we list the first few examples:

$$\int X\, F(\vec{r},\vec{v})d^3r = f_1^1(E); \tag{53a}$$

$$\int Y\, F(\vec{r},\vec{v})d^3r = \int Z\, F(\vec{r},\vec{v})d^3r = 0; \tag{53b}$$

$$\int X^2\, F(\vec{r},\vec{v})d^3r = \tfrac{1}{3}f_0^2(E) + \tfrac{2}{3}f_2^2(E); \tag{53c}$$

$$\int Y^2\, F(\vec{r},\vec{v})d^3r = \int Z^2\, F(\vec{r},\vec{v})d^3r = \tfrac{1}{3}f_0^2(E) - \tfrac{1}{3}f_2^2(E); \tag{53d}$$

$$\int XY\, F(\vec{r},\vec{v})d^3r = 0; \tag{53e}$$

$$\int X^3\, F(\vec{r},\vec{v})d^3r = \tfrac{3}{5}f_1^3(E) + \tfrac{2}{5}f_3^3(E); \tag{53f}$$

$$\int XY^2 F(\vec{r},\vec{v})d^3r = \tfrac{1}{5}f_1^3(E) - \tfrac{1}{5}f_3^3(E); \tag{53g}$$

etc.

Again, of course, by adding a number of indices we could easily generalize these results to the more complex cases of an impurity ion or a polyatomic medium.

5. Evaluation for Power Cross Sections

LINDHARD et al. (1963b) have shown that moments over the range distribution can be calculated by exact integration if the power cross section (5) is used. SANDERS (1968) has shown that the same is true for moments over the damage distribution, and some numerical results have been presented in an earlier communication (SIGMUND & SANDERS, 1967). In this section we first discuss the method and then present some numerical results.

First Order Moments: Equal Mass Case

Equation (44) reads, for $n = l = 1$,

$$F_0^0(E) + 2F_2^0(E) = 3N \int d\sigma \left[F_1^1(E) - \cos\varphi' \, F_1^1(E - T) - \cos\varphi'' F_1^1(T) \right]$$

or, after inserting the cross section $d\sigma$ from (5), the zero order moments from (45) and the laboratory scattering angles

$$\cos\varphi' = (1 - T/E)^{1/2}, \cos\varphi'' = (T/E)^{1/2}, \tag{54}$$

$$\left. \begin{aligned} E = 3NCE^{-m} \int_0^E T^{-1-m} dT \left[F_1^1(E) - (1 - T/E)^{1/2} F_1^1(E - T) \right. \\ \left. - (T/E)^{1/2} F_1^1(T) \right]. \end{aligned} \right\} \tag{55}$$

Before solving (55) we investigate the boundary conditions imposed by a threshold energy W, as introduced in sect. 3. For planar geometry, and neglecting the energy loss U for the moment, we have

$$F(x, \vec{v}) = E\delta(x) \quad \text{for} \quad E \leq W, \tag{56}$$

so, by use of (38) and (43),

$$F_l^n(E) = \delta_{l0} \delta_{n0} E \quad \text{for} \quad E \leq W, \tag{57}$$

i.e. $F_1^1(E) = 0$ for $E \leq W$.

We first treat the case $W = 0$. With the *ansatz*

$$F_1{}^1(E) = \frac{A_1{}^1}{NC} E^{1+2m} \tag{58}$$

where $A_1{}^1$ is a constant, we obtain from (55)

$$1 = 3A_1{}^1 \int_0^1 t^{-1-m} dt \,[1 - (1-t)^{3/2+2m} - t^{3/2+2m}],$$

where now

$$t = T/E. \tag{59}$$

The integrals are easily evaluated and yield

$$3A_1{}^1 = \left[-\frac{1}{m} - B(-m, 5/2+2m) - \frac{1}{3/2+m} \right]^{-1} \tag{60}$$

$B(x,y)$ is the beta function (ABRAMOWITZ & STEGUN, 1964),

$$B(x,y) = \int_0^1 dt \, t^{x-1}(1-t)^{y-1} = \frac{\Gamma(x)\,\Gamma(y)}{\Gamma(x+y)}. \tag{61}$$

Because of (45) all other moments $F_l{}^1(E)$ are zero so, by use of (43) and (36), we obtain the "average damage depth"

$$\langle x \rangle = \frac{\int x \, dx \, F(x,\vec{v})}{\int dx \, F(x,\vec{v})} = \frac{3A_1{}^1}{NC} E^{2m} \cos\theta, \tag{62}$$

where θ is the angle between the beam and the x-axis.

This is to be compared with the average projected range that was first calculated by LINDHARD et al. (1963b) and is, in the present notation,

$$\langle x \rangle_{(R)} = \frac{3A_{(R)1}{}^1}{NC} E^{2m} \cos\theta,$$

where

$$3A_{(R)1}{}^1 = \left[-\frac{1}{m} - B(-m, 3/2+2m) \right]^{-1}$$

Note that, because of the different normalization condition of the range distribution, we have

$$F_{(R)1}{}^1(E) = \frac{A_{(R)1}{}^1}{NC} E^{2m},$$

i. e. an energy dependence that is different from that in (58).

We now consider the case $W > 0$. It is then no longer possible to calculate the complete $F_1{}^1(E)$ explicitly, but the asymptotic form for $E \gg W$ can be found by Laplace transform, as was shown by ROBINSON (1965a) on a similar integral equation. Introducing the logarithmic variable $u = \ln E/W$ in (55) we obtain, by following Robinson's method, the following expression for the Laplace transform $\bar{F}_1^1(s)$ of $F_1^1(E(u))$ with respect to u:

$$\bar{F}_1{}^1(s) = -\frac{mW^{1+2m}}{3NC} \frac{1}{(s-1-2m)(1-2\bar{g}(s+1/2))}, \tag{63}$$

where

$$\bar{g}(s) = -\frac{m}{2} \cdot \frac{1}{s-m} + \frac{1}{2} \frac{\Gamma(1-m)\,\Gamma(s+1)}{\Gamma(s+1-m)}.$$

It appears difficult to express the inverse Laplace transform of (63) in terms of elementary functions, but it is easy to evaluate the first two terms in an asymptotic expansion in powers of E/W. These arise from the two poles at $s = 1 + 2m$ and $s = 1/2$ in (63). We then obtain

$$F_1{}^1(E) \sim \frac{A_1{}^1}{NC} E^{1+2m} - \frac{\tilde{A}_1{}^1}{NC} E^{1/2} W^{1/2+2m} \quad \text{for} \quad E \gg W, \tag{64}$$

where $A_1{}^1$ is identical with the expression calculated before, eq. (60), and

$$3\tilde{A}_1{}^1 = \frac{m(1-m)}{1/2+2m} \cdot \frac{1}{\psi(1)-\psi(1-m)}, \tag{64a}$$

$\psi(x) = \dfrac{d}{dx} \ln \Gamma(x)$. Thus the first correction term for $W \neq 0$ is smaller where than the main term by a factor of the order of $(W/E)^{1/2+2m}$. For $m > 1/4$ this factor goes more rapidly to zero than W/E. This means that W can usually be neglected when E is in the keV region, and the error made can be estimated from eq. (64).

A similar calculation shows that the correction in the average projected range due to a threshold W is proportional to $E^{-1/2}$, i. e. again smaller by a factor of the order of $(W/E)^{1/2+2m}$ than the leading term. Of course the numerical factor $\tilde{A}_1{}^1$ is different from the one given by (64a).

Introduction of an energy loss U of the recoiling atoms, as discussed in § 3, has two consequences. First, since energy is not conserved, the left-hand side of eq. (55) is replaced by $E - \Delta E$. Because of eq. (29a), this means that for $E \gg U, W$, the left-hand side of eq. (55) remains linear in E. Hence, because of eq. (62), the average $\langle x \rangle$ is not affected. Second, the recoil term $F_1^1(T)$ in eq. (55) is replaced by $F_1^1(T - U)$. It is, then, possible to establish an asymptotic expansion of $F_1^1(E)$ in powers of U/E, where (62) is the leading term. Higher terms can be neglected for $E \gg U$.

First Order Moments: Nonequal Mass Case

Equation (46) reads, for $n = l = 1$,

$$E = 3N \int d\sigma_{(1)} [F_{(1)1}^1(E) - \cos\varphi_{(1)}{}' F_{(1)1}^1(E - T) - \cos\varphi_{(1)}{}'' F_1^1(T)], \quad (65)$$

where (47) has been inserted on the left side. The laboratory scattering angles $\varphi_{(1)}{}'$ and $\varphi_{(1)}{}''$ are given by

$$\cos\varphi_{(1)}{}' = (1 - T/E)^{1/2} + \alpha \frac{T}{E}(1 - T/E)^{-1/2} \quad (66\,a)$$

and

$$\cos\varphi_{(1)}{}'' = \gamma^{-1/2}(T/E)^{1/2} \quad (66\,b)$$

for elastic collisions, where

$$\alpha = \frac{1}{2}(1 - M_2/M_1). \quad (66\,c)$$

The cross section $d\sigma_{(1)}$ is given by

$$d\sigma_{(1)} = C_{(1)} E^{-m_{(1)}} T^{-1-m_{(1)}} dT, \quad 0 \le T \le \gamma E \quad (67)$$

where in general, $C_{(1)}$ and $m_{(1)}$ are different from C and m. We shall assume in the following that

$$m_{(1)} = m, \quad (68)$$

i. e. the same power in the cross section for both types of interaction. This is a gross simplification, the validity of which will be discussed in the following chapter. Accepting (68) for the moment, we can make the *ansatz*

$$F_{(1)1}^1(E) = \frac{A_{(1)1}^1}{NC_{(1)}} E^{1+2m} \quad (69)$$

and, inserting both (58) and (69) into (65), we obtain

$$1 + \frac{3}{3/2 + m} A_1{}^1 \frac{C_{(1)}}{C} \gamma^{1+m} = 3A_{(1)1}{}^1 \int_0^\gamma \frac{dt}{t^{1+m}} [1 - \cos\varphi_{(1)}'(1-t)^{1+2m}]. \quad (69\,a)$$

The integral is easily evaluated after inserting (66a) and we get

$$1 + \frac{3}{3/2 + m} A_1{}^1 \frac{C_{(1)}}{C} \gamma^{1+m} = 3A_{(1)1}{}^1 \left\{ -\frac{\gamma^{-m}}{m} - B_\gamma(-m, 5/2 + 2m) \right. \\ \left. - \alpha B_\gamma(1 - m, 3/2 + 2m) \right\}, \quad (70$$

where B_γ is the incomplete beta function,

$$B_\gamma(x, y) = \int_0^\gamma dt\, t^{x-1}(1-t)^{y-1}. \quad (71)$$

Eq. (70) determines $A_{(1)1}{}^1$, since $A_1{}^1$, $C_{(1)}$, and C are known. We note that from (5 a)

$$\frac{C_{(1)}}{C} = \left(\frac{M_1}{M_2}\right)^m \left(\frac{Z_1}{Z_2}\right)^{2m} \left(\frac{a_{12}}{a_{22}}\right)^{2(1-m)}$$

or, with the approximation $Z_2/Z_1 = M_2/M_1 = \mu$,

$$\frac{C_{(1)}}{C} = \mu^{-3m} \left(\frac{2}{1 + \mu^{-2/3}}\right)^{1-m}. \quad (72)$$

It may be appropriate to make a remark on the convergence of the above integrals. Eq. (70) follows directly from (69 a) provided $m < 0$ so that each term in the integral converges. For $0 < m < 1$, it is readily verified that the integral as a whole converges, while divergences occur in two terms at $t = 0$. The divergence can easily be removed by partial integration, but this would make (70) look more complicated. Instead we understand (70) for $0 < m < 1$ as the analytical continuation from the region $m < 0$.

First Order Moments: Two Different Power Cross Sections

There is no basic obstacle against treating the case $m \neq m_{(1)}$, and in fact, the solutions of (65) can be found by straightforward calculation. However, it is highly desirable to make use of the simple power laws of the type of (69), as long as this can be justified. The main advantage is, as has been seen, that *all lengths* are proportional to $E^{2m}/NC_{(1)}$ and there is complete similarity of all distributions over the

energy range where the power cross section in question is valid, so that the only numerical work to be done is the calculation of various factors. In the case $m \neq m_{(1)}$, (69) is no longer valid.

Let us assume a primary particle 1 with energy E that slows down by a power cross section characterized by $m_{(1)}$. Recoil atoms have energies T up to $T_m = \gamma E$. There is formally no lower limit for T, but for the stopping only recoils with, say $T \gtrsim \frac{1}{100} T_m$ are important. Thus

$$\frac{1}{100} \gamma E < T < \gamma E \tag{73}$$

is the energy range of interest for recoiling atoms whose scattering is characterized by a power m in the cross section. Whether eq. (68) is a reasonable assumption depends on the values of T and E in dimensionless units. We introduce two different energy units,

$$\varepsilon = E \frac{M_2}{M_1 + M_2} \frac{a_{12}}{Z_1 Z_2 e^2}; \quad \tau = T \frac{1}{2} \frac{a_{22}}{Z_2^2 e^2}, \tag{73a}$$

which both follow from (1a), τ applying to the equal-mass case. Hence (73) reads

$$\frac{1}{100} \varepsilon \varkappa(\mu) < \tau < \varepsilon \cdot \varkappa(\mu), \tag{74}$$

where

$$\varkappa(\mu) \approx \frac{2}{\mu(1 + \mu)} \sqrt{\tfrac{1}{2}(1 + \mu^{-2/3})} \tag{74a}$$

and $\mu = M_2/M_1 \approx Z_2/Z_1$. Figure 4 shows that the function $\varkappa(\mu)$ varies rapidly with μ, so that primary and recoil energies can differ by several orders of magnitude when measured in dimensionless units. Now, let us first assume that $M_2/M_1 < 1$, say $M_2/M_1 = 1/4$ so $\varkappa(\mu) = 8.5$, according to Fig. 4. Then $0.1 \varepsilon \lesssim \tau < 8.5 \varepsilon$. Hence the distribution of τ values centres around ε on a logarithmic scale, with a spread of a factor of 10 to both sides. Thus one seems justified in assuming that primary and secondary particles obey similar scattering laws, $m \approx m_{(1)}$. If M_2/M_1 is considerably smaller than 1/4 the ratio τ/ε will be greater. Thus in extreme cases it may become necessary to assume $m > m_{(1)}$. Let us now assume $M_2/M_1 > 1$, say $M_2/M_1 = 4$, or $\varkappa(\mu) = 0.083$. Obviously the distribution of τ values ranges from $\sim 0.1 \varepsilon$ down to $\sim 0.001 \varepsilon$, i.e. we will have in general $m < m_{(1)}$ for $M_1 \ll M_2$. However for $M_1 \ll M_2$ the ranges of recoiling atoms are small, so the recoil term is negligible. This can be seen from the fact that the term containing the factor $C_{(1)}/C$ in (69a) goes to zero as μ^{-1-4m} for $\mu \gg 1$.

We conclude that assumption (68) is justified for $M_1 \gg M_2$, while for $M_1 \ll M_2$ the choice of m does not affect the calculated quantities. For $M_1 \approx M_2$ neither argument applies. Therefore we consider the case $M_1 = M_2$ more quantitatively. Going back to (55), one way to solve the problem would be to assume that the primary particle of energy E has a scattering law with $m = m_1$, and secondary particles, with energy T, have $m = m_2$, where $m_2 < m_1$ since $T < E$. This is, however, unsatisfactory, because a measurable fraction of all recoil atoms do have energies of the order of E. Instead, we assume the following consistent picture: introduce an arbitrary energy E_1 and assume that whenever an atom (primary or secondary)
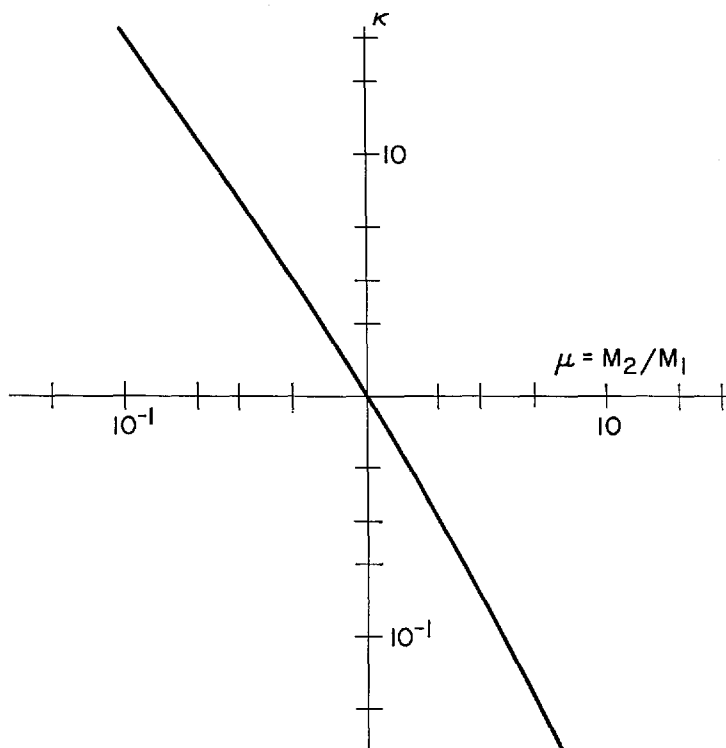
Fig. 4. The function $\varkappa(\mu)$ defined in (74a), as a function of mass ratio.

has an energy below E_1 the cross section is given by $m = m_1$, while for energies $> E_1$ we have $m = m_2$ ($> m_1$). Then, of course, $F_1{}^1(E)$ is given by (58) for $E < E_1$, with $C = C_1$ and $m = m_1$ in (60). For $E > E_1$, the integrations in (55) have to be split into the regions $E \gtrless E_1$, and $F_1{}^1(E)$ inserted as a known inhomogeneity for $E \leq E_1$. Eq. (55) can then be solved by Laplace transform, just as in the first chapter of this section, with E_1 substituted for W. The resulting expression contains (58) as the leading term with the highest power of E with $m = m_2$ and $C = C_2$, while the first correction term goes as $E^{1/2}$, i.e. can usually be neglected in comparison with $E^{1 + 2m_2}$. Thus (58) holds both for $E < E_1$ and $E > E_1$, with the respective value of m inserted in each energy region. Since this is just what was assumed above we conclude that even in the case $M_1 = M_2$, where the assumption (68) was least justified, one is indeed allowed to make it. The result of this paragraph may seem trivial to the reader, but one should be cautious. There are other, similar integral equations (SIGMUND, 1969a, 1969b) where exactly the opposite result is true. The choice of the power m is a major problem that has to be considered with great care whenever power cross sections are used.

Higher Order Moments

Higher order moments ($n \geq 2$) can be calculated in a similar way as first order ones. We set $W = U = 0$ from the beginning—which choice could be justified in the same way as for $n = 1$—and also choose a single power m in the cross sections $d\sigma$ and $d\sigma_{(1)}$.

Equal-Mas Case

Equation (44) reads, with the cross section (5),

$$\left. \Delta F_l^n(E) = (2l+1)NC E^{-2m} \int_0^1 \frac{dt}{t^{1+m}} [F_l^n(E) - P_l(\cos\varphi')F_l^n(E(1-t)) \right. \\ \left. - P_l(\cos\varphi'')F_l^n(El)], \right\} \quad (75)$$

where

$$\Delta F_l^n(E) = nlF_{l-1}^{n-1}(E) + n(l+1)F_{l+1}^{n-1}(E). \quad (75\,\mathrm{a})$$

With the *ansatz*

$$F_l^n(E) = A_l^n E\left(\frac{E^{2m}}{NC}\right)^n, \quad (76)$$

(45) becomes

$$A_l^0 = \delta_{l0}, \quad (76\mathrm{a})$$

and (75) gives

$$A_l^n = \frac{\Delta A_l^n}{(2l+1)I_l^n}, \quad (77)$$

where

$$I_l^n = \int_0^1 \frac{dt}{t^{1+m}} [1 - P_l(\sqrt{1-t})(1-t)^{2mn+1} - P_l(\sqrt{t})t^{2mn+1}]. \quad (77\,\mathrm{a})$$

ΔA_l^n is defined in analogy to (75 a),

$$\Delta A_l^n = nlA_{l-1}^{n-1} + n(l+1)A_{l+1}^{n-1}. \quad (77\,\mathrm{b})$$

Thus it depends only on the $A_{l'}^{n-1}$. Hence the problem has been reduced to evaluating the integrals I_l^n. As before it is easily verified that I_l^n as a whole is convergent for $m < 1$, so it is legitimate to evaluate I_l^n first for $m < 0$, where each of the three terms is finite, and then continue the result to the region $0 \leq m < 1$.

For $m < 0$ we can write

$$I_l^n = -\frac{1}{m} - J_l^n - K_l^n \tag{78}$$

where

$$J_l^n = \int_0^1 \frac{dt}{t^{1+m}} P_l(\sqrt{1-t})(1-t)^{2mn+1}, \tag{78a}$$

and

$$K_l^n = \int_0^1 \frac{dt}{t^{1+m}} P_l(\sqrt{t}) t^{2mn+1}. \tag{78b}$$

The two integrals are reduced to readily calculable forms in Appendix A. It should be mentioned that in a previous communication (SIGMUND & SANDERS, 1967) we evaluated J_l^n and K_l^n in "the pedestrian way", i.e. by inserting P_l, and evaluating the resulting beta functions, first for $n \le 3$ and later for $n \le 5$. This is perfectly justified for small n. In the present work we evaluate A_l^n up to $n = 20$ and in this case one has to make the accumulation of errors in the recurrence procedure as small as possible. The method described in Appendix A is one of several procedures that have been tried. Since it is the simplest one, we have confidence that the results are accurate. In the most important lower moments ($n \le 3$) agreement is found between the results computed by various methods and our previous results obtained with the desk calculator.

Non-Equal Masses

With the cross section $d\sigma_{(1)} = C_{(1)} E^{-m} T^{-1-m} dT$, (46) reads

$$\left. \begin{aligned} \Delta F_{(1)l}^n(E) = (2l+1)NC_{(1)}E^{-2m} \int_0^\gamma \frac{dt}{t^{1+m}} [F_{(1)l}^n(E) - P_l(\cos\varphi_{(1)}') \times \\ \times F_{(1)l}^n(E(1-t)) - P_l(\cos\varphi_{(1)}'')F_l^n(Et)] \end{aligned} \right\} \tag{79}$$

Inserting (76) in the last term on the right side we obtain, with the *ansatz*

$$F_{(1)l}^n(E) = A_{(1)l}^n E\left(\frac{E^{2m}}{NC_{(1)}}\right)^n, \tag{80}$$

$$d_l^n A_{(1)l}^n = \frac{\Delta A_{(1)l}^n}{2l+1} + A_l^n \left(\frac{C_{(1)}}{C}\right)^n \mathscr{K}_l^n, \tag{81}$$

3*

where

$$d_l{}^n = -\frac{\gamma^{-m}}{m} - \mathscr{J}_l{}^n, \tag{81 a}$$

$$\mathscr{J}_l{}^n = \int_0^\gamma \frac{dt}{t^{1+m}} P_l(\cos\varphi_{(1)}')(1-t)^{2mn+1}, \tag{81 b}$$

and

$$\mathscr{K}_l{}^n = \int_0^\gamma dt\, t^{m(2n-1)} P_l(\cos\varphi_{(1)}''). \tag{81 c}$$

From (78 b) and (81 c), (75 b) and (79 a), we get

$$\mathscr{K}_l{}^n = \gamma^{1+m(2n-1)} K_l{}^n. \tag{82}$$

Also, from (47)

$$A_{(1)l}{}^0 = \delta_{l0}. \tag{83}$$

Thus, given the $A_l{}^n$, the computation of $A_{(1)l}{}^n$ is reduced to evaluating integrals. The $\mathscr{J}_l{}^n$ are evaluated in Appendix A.

Range Calculations

Moments over the ion range are calculated with the same program, the differences being the following:

i) There are no $K_l{}^n$ or $\mathscr{K}_l{}^n$ terms, since the recoil term is absent in (25). Hence it is not necessary first to evaluate the equal-mass case.

ii) Because of the different normalization condition (24), the exponents of $(1-t)$ in (78 a) and (81 b) are $2mn$, instead of $2mn+1$. The extra factor E in (76) and (80) disappears.

Polyatomic Targets

The extension to polyatomic targets is easily done by adding the appropriate indices and summing over the various components. Because of the difference in the values of ε, power cross sections are not applicable when the constituents of the target have extremely different masses. Consider (28 a). We define

$$N_i = \alpha_i N, \tag{84}$$

so that α_i is the fraction of atoms of type i ($i = 2, 3 \ldots$). Following the procedure of the previous sections we obtain the following expression for the moments over the function $F_{(i)}(\bar{r}, \bar{v})$:

Nr. 14

TABLE I. Coefficients A_l^n, defined by (76), for $M_1 = M_2$ and various values of m. (Note that in case of the *range* distribution the extra factor E in (76) has to be dropped).

(Ia) Deposited Energy: Nonvanishing Coefficients A_l^n for $n \leq 5$.

	$m = 2/3$	$m = 1/2$	$m = 1/3$	$m = 1/4$	$m = 1/8$	$m = 1/16$
A_0^0	1.000	1.000	1.000	1.000	1.000	1.000
A_1^1	$5.199_{10^{-2}}$	$9.831_{10^{-2}}$	$1.685_{10^{-1}}$	$2.188_{10^{-1}}$	$3.307_{10^{-1}}$	$4.170_{10^{-1}}$
A_0^2	$1.297_{10^{-2}}$	$4.916_{10^{-2}}$	$1.572_{10^{-1}}$	$2.871_{10^{-1}}$	$8.777_{10^{-1}}$	2.149
A_2^2	$3.921_{10^{-3}}$	$1.419_{10^{-2}}$	$4.043_{10^{-2}}$	$6.563_{10^{-2}}$	$1.349_{10^{-1}}$	$1.958_{10^{-1}}$
A_1^3	$1.880_{10^{-3}}$	$1.415_{10^{-2}}$	$7.813_{10^{-2}}$	$1.830_{10^{-1}}$	$8.195_{10^{-1}}$	2.517
A_3^3	$3.404_{10^{-4}}$	$2.420_{10^{-3}}$	$1.153_{10^{-2}}$	$2.320_{10^{-2}}$	$6.275_{10^{-2}}$	$1.017_{10^{-1}}$
A_0^4	$6.100_{10^{-4}}$	$9.583_{10^{-3}}$	$9.911_{10^{-2}}$	$3.203_{10^{-1}}$	2.689	$1.485_{10^{1}}$
A_2^4	$2.644_{10^{-4}}$	$4.021_{10^{-3}}$	$3.815_{10^{-2}}$	$1.126_{10^{-1}}$	$6.853_{10^{-1}}$	2.408
A_4^4	$3.158_{10^{-5}}$	$4.530_{10^{-4}}$	$3.662_{10^{-3}}$	$9.162_{10^{-3}}$	$3.254_{10^{-2}}$	$5.880_{10^{-2}}$
A_1^5	$1.275_{10^{-4}}$	$4.169_{10^{-3}}$	$7.686_{10^{-2}}$	$3.217_{10^{-1}}$	3.979	$2.763_{10^{1}}$
A_3^5	$3.615_{10^{-5}}$	$1.132_{10^{-3}}$	$1.856_{10^{-2}}$	$6.857_{10^{-2}}$	$5.513_{10^{-1}}$	2.145
A_5^5	$3.031_{10^{-6}}$	$8.992_{10^{-5}}$	$1.256_{10^{-3}}$	$3.933_{10^{-3}}$	$1.852_{10^{-2}}$	$3.765_{10^{-2}}$

(Ib) Range: Nonvanishing Coefficients A_l^n, for $n \leq 5$.

	$m = 2/3$	$m = 1/2$	$m = 1/3$	$m = 1/4$	$m = 1/8$	$m = 1/16$
A_0^0	1.000	1.000	1.000	1.000	1.000	1.000
A_1^1	$6.799_{10^{-2}}$	$1.229_{10^{-1}}$	$1.991_{10^{-1}}$	$2.500_{10^{-1}}$	$3.562_{10^{-1}}$	$4.336_{10^{-1}}$
A_0^2	$2.072_{10^{-2}}$	$7.374_{10^{-2}}$	$2.168_{10^{-1}}$	$3.750_{10^{-1}}$	1.031	2.352
A_2^2	$5.881_{10^{-3}}$	$1.993_{10^{-2}}$	$5.229_{10^{-2}}$	$8.077_{10^{-2}}$	$1.519_{10^{-1}}$	$2.089_{10^{-1}}$
A_1^3	$3.339_{10^{-3}}$	$2.331_{10^{-2}}$	$1.166_{10^{-1}}$	$2.561_{10^{-1}}$	1.010	2.840
A_3^3	$5.559_{10^{-4}}$	$3.650_{10^{-3}}$	$1.574_{10^{-2}}$	$2.984_{10^{-2}}$	$7.251_{10^{-2}}$	$1.101_{10^{-1}}$
A_0^4	$1.211_{10^{-3}}$	$1.755_{10^{-2}}$	$1.626_{10^{-1}}$	$4.889_{10^{-1}}$	3.533	$1.748_{10^{1}}$
A_2^4	$5.044_{10^{-4}}$	$7.051_{10^{-3}}$	$5.986_{10^{-2}}$	$1.645_{10^{-1}}$	$8.698_{10^{-1}}$	2.770
A_4^4	$5.468_{10^{-5}}$	$7.167_{10^{-4}}$	$5.176_{10^{-3}}$	$1.211_{10^{-2}}$	$3.815_{10^{-2}}$	$6.415_{10^{-2}}$
A_1^5	$2.706_{10^{-4}}$	$8.110_{10^{-3}}$	$1.329_{10^{-1}}$	$5.145_{10^{-1}}$	5.414	$3.333_{10^{1}}$
A_3^5	$7.258_{10^{-5}}$	$2.073_{10^{-3}}$	$3.010_{10^{-2}}$	$1.030_{10^{-1}}$	$7.125_{10^{-1}}$	2.497
A_5^5	$5.476_{10^{-6}}$	$1.472_{10^{-4}}$	$1.818_{10^{-3}}$	$5.291_{10^{-3}}$	$2.190_{10^{-2}}$	$4.123_{10^{-2}}$

TABLE II. Coefficients $A_{(1)l}^n$, defined by (80), as functions of mass ratio M_2/M_1.

(IIa) Deposited Energy: $m = 1/2$.

M_2/M_1	1/10	1/4	1/2	1	2	4	10
$A_{(1)0}^{0}$	1.000	1.000	1.000	1.000	1.000	1.000	1.000
$A_{(1)1}^{1}$	$2.305_{10^{-1}}$	$1.630_{10^{-1}}$	$1.254_{10^{-1}}$	$9.831_{10^{-2}}$	$8.020_{10^{-2}}$	$6.588_{10^{-2}}$	$4.761_{10^{-2}}$
$A_{(1)0}^{2}$	$2.905_{10^{-1}}$	$1.434_{10^{-1}}$	$7.978_{10^{-2}}$	$4.916_{10^{-2}}$	$3.801_{10^{-2}}$	$3.376_{10^{-2}}$	$3.077_{10^{-2}}$
$A_{(1)2}^{2}$	$8.032_{10^{-2}}$	$4.008_{10^{-2}}$	$2.328_{10^{-2}}$	$1.419_{10^{-2}}$	$9.266_{10^{-3}}$	$5.929_{10^{-3}}$	$2.890_{10^{-3}}$
$A_{(1)1}^{3}$	$2.374_{10^{-1}}$	$7.864_{10^{-2}}$	$3.009_{10^{-2}}$	$1.415_{10^{-2}}$	$9.386_{10^{-3}}$	$7.001_{10^{-3}}$	$4.601_{10^{-3}}$
$A_{(1)3}^{3}$	$3.521_{10^{-2}}$	$1.216_{10^{-2}}$	$5.180_{10^{-3}}$	$2.420_{10^{-3}}$	$1.236_{10^{-3}}$	$5.967_{10^{-4}}$	$1.911_{10^{-4}}$
$A_{(1)0}^{4}$	$5.923_{10^{-1}}$	$1.231_{10^{-1}}$	$2.802_{10^{-2}}$	$9.583_{10^{-3}}$	$6.256_{10^{-3}}$	$4.976_{10^{-3}}$	$3.911_{10^{-3}}$
$A_{(1)2}^{4}$	$2.137_{10^{-1}}$	$4.591_{10^{-2}}$	$1.148_{10^{-2}}$	$4.021_{10^{-3}}$	$2.196_{10^{-3}}$	$1.288_{10^{-3}}$	$5.693_{10^{-4}}$
$A_{(1)4}^{4}$	$1.833_{10^{-2}}$	$4.257_{10^{-3}}$	$1.283_{10^{-3}}$	$4.530_{10^{-4}}$	$1.776_{10^{-4}}$	$6.348_{10^{-5}}$	$1.321_{10^{-5}}$

(IIb) Deposited Energy: $m = 1/3$.

M_2/M_1	1/10	1/4	1/2	1	2	4	10
$A_{(1)0}^{0}$	1.000	1.000	1.000	1.000	1.000	1.000	1.000
$A_{(1)1}^{1}$	$3.776_{10^{-1}}$	$2.678_{10^{-1}}$	$2.123_{10^{-1}}$	$1.685_{10^{-1}}$	$1.338_{10^{-1}}$	$1.074_{10^{-1}}$	$8.056_{10^{-2}}$
$A_{(1)0}^{2}$	$6.347_{10^{-1}}$	$3.573_{10^{-1}}$	$2.382_{10^{-1}}$	$1.572_{10^{-1}}$	$1.142_{10^{-1}}$	$1.002_{10^{-1}}$	$8.842_{10^{-3}}$
$A_{(1)2}^{2}$	$2.078_{10^{-1}}$	$1.032_{10^{-1}}$	$6.468_{10^{-2}}$	$4.043_{10^{-2}}$	$2.529_{10^{-2}}$	$1.605_{10^{-2}}$	$2.764_{10^{-2}}$
$A_{(1)1}^{3}$	$6.364_{10^{-1}}$	$2.701_{10^{-1}}$	$1.468_{10^{-1}}$	$7.813_{10^{-2}}$	$4.742_{10^{-2}}$	$3.504_{10^{-2}}$	$1.127_{10^{-3}}$
$A_{(1)3}^{3}$	$1.387_{10^{-1}}$	$4.790_{10^{-2}}$	$2.359_{10^{-2}}$	$1.153_{10^{-2}}$	$5.632_{10^{-3}}$	$2.805_{10^{-3}}$	$4.987_{10^{-2}}$
$A_{(1)0}^{4}$	1.359	$4.911_{10^{-1}}$	$2.246_{10^{-1}}$	$9.911_{10^{-2}}$	$5.755_{10^{-2}}$	$4.713_{10^{-2}}$	$6.325_{10^{-3}}$
$A_{(1)2}^{4}$	$6.473_{10^{-1}}$	$2.046_{10^{-1}}$	$8.983_{10^{-2}}$	$3.815_{10^{-2}}$	$1.878_{10^{-2}}$	$1.111_{10^{-2}}$	$1.583_{10^{-4}}$
$A_{(1)4}^{4}$	$1.048_{10^{-1}}$	$2.507_{10^{-2}}$	$9.650_{10^{-3}}$	$3.662_{10^{-3}}$	$1.390_{10^{-3}}$	$5.413_{10^{-4}}$	

$$F_{(i)l}^n(E) = G_{(i)l}^n E\left(\frac{E^{2m}}{N\overline{C}}\right)^n, \tag{85}$$

where $\overline{C}$ is an average C value defined in some arbitrary way, and the $G_{(i)l}^n$ are found from the following system of equations:

$$\frac{\Delta G_{(i)l}^n}{2l+1} = \sum_k \alpha_k \frac{C_{(ik)}}{\overline{C}}\{G_{(i)l}^n d_{(ik)l}^n - G_{(k)l}^n \mathscr{K}_{(ik)l}^n\}. \tag{85a}$$

TABLE II (continued). Coefficients $A_{(1)l}{}^n$, defined by (80), as functions of mass ratio M_2/M_1.

(IIc) Range, $m = 1/2$.

M_2/M_1	1/10	1/4	1/2	1	2	4	10
$A_{(1)0}{}^0$	1.000	1.000	1.000	1.000	1.000	1.000	1.000
$A_{(1)1}{}^1$	$2.805_{10^{-1}}$	$1.922_{10^{-1}}$	$1.511_{10^{-1}}$	$1.229_{10^{-1}}$	$9.904_{10^{-2}}$	$7.623_{10^{-2}}$	$5.090_{10^{-2}}$
$A_{(1)0}{}^2$	$2.582_{10^{-1}}$	$1.345_{10^{-1}}$	$9.404_{10^{-2}}$	$7.374_{10^{-2}}$	$6.166_{10^{-2}}$	$5.333_{10^{-2}}$	$4.684_{10^{-2}}$
$A_{(1)2}{}^2$	$9.840_{10^{-2}}$	$4.794_{10^{-2}}$	$3.031_{10^{-2}}$	$1.993_{10^{-2}}$	$1.255_{10^{-2}}$	$7.226_{10^{-3}}$	$3.154_{10^{-3}}$
$A_{(1)1}{}^3$	$1.454_{10^{-1}}$	$5.743_{10^{-2}}$	$3.433_{10^{-2}}$	$2.331_{10^{-2}}$	$1.655_{10^{-2}}$	$1.162_{10^{-2}}$	$7.109_{10^{-3}}$
$A_{(1)3}{}^3$	$3.838_{10^{-2}}$	$1.362_{10^{-2}}$	$6.963_{10^{-3}}$	$3.650_{10^{-3}}$	$1.759_{10^{-3}}$	$7.457_{10^{-4}}$	$2.106_{10^{-4}}$
$A_{(1)0}{}^4$	$1.479_{10^{-1}}$	$4.769_{10^{-2}}$	$2.644_{10^{-2}}$	$1.755_{10^{-2}}$	$1.275_{10^{-2}}$	$9.649_{10^{-3}}$	$7.229_{10^{-3}}$
$A_{(1)2}{}^4$	$8.062_{10^{-2}}$	$2.443_{10^{-2}}$	$1.237_{10^{-2}}$	$7.051_{10^{-3}}$	$4.044_{10^{-3}}$	$2.179_{10^{-3}}$	$8.829_{10^{-4}}$
$A_{(1)4}{}^4$	$1.605_{10^{-2}}$	$4.212_{10^{-3}}$	$1.739_{10^{-3}}$	$7.167_{10^{-4}}$	$2.602_{10^{-4}}$	$8.050_{10^{-5}}$	$1.463_{10^{-5}}$

(IId) Range, $m = 1/3$.

M_2/M_1	1/10	1/4	1/2	1	2	4	10
$A_{(1)0}{}^0$	1.000	1.000	1.000	1.000	1.000	1.000	1.000
$A_{(1)1}{}^1$	$6.511_{10^{-1}}$	$3.821_{10^{-1}}$	$2.685_{10^{-1}}$	$1.991_{10^{-1}}$	$1.520_{10^{-1}}$	$1.170_{10^{-1}}$	$8.384_{10^{-2}}$
$A_{(1)0}{}^2$	1.394	$5.402_{10^{-1}}$	$3.123_{10^{-1}}$	$2.168_{10^{-1}}$	$1.768_{10^{-1}}$	$1.653_{10^{-1}}$	$1.795_{10^{-1}}$
$A_{(1)2}{}^2$	$5.226_{10^{-1}}$	$1.852_{10^{-1}}$	$9.388_{10^{-2}}$	$5.229_{10^{-2}}$	$3.046_{10^{-2}}$	$1.805_{10^{-2}}$	$9.315_{10^{-3}}$
$A_{(1)1}{}^3$	1.795	$4.523_{10^{-1}}$	$2.045_{10^{-1}}$	$1.166_{10^{-1}}$	$7.872_{10^{-2}}$	$5.945_{10^{-2}}$	$4.670_{10^{-2}}$
$A_{(1)3}{}^3$	$4.609_{10^{-1}}$	$1.009_{10^{-1}}$	$3.747_{10^{-2}}$	$1.574_{10^{-2}}$	$6.995_{10^{-3}}$	$3.200_{10^{-3}}$	$1.194_{10^{-3}}$
$A_{(1)0}{}^4$	4.194	$7.552_{10^{-1}}$	$2.978_{10^{-1}}$	$1.626_{10^{-1}}$	$1.146_{10^{-1}}$	$9.926_{10^{-2}}$	$1.092_{10^{-1}}$
$A_{(1)2}{}^4$	2.250	$3.735_{10^{-1}}$	$1.314_{10^{-1}}$	$5.986_{10^{-2}}$	$3.206_{10^{-2}}$	$1.888_{10^{-2}}$	$1.060_{10^{-2}}$
$A_{(1)4}{}^4$	$4.318_{10^{-1}}$	$5.946_{10^{-2}}$	$1.631_{10^{-2}}$	$5.176_{10^{-3}}$	$1.758_{10^{-3}}$	$6.226_{10^{-4}}$	$1.682_{10^{-4}}$

The quantities $d_{(ik)l}{}^n$ and $\mathcal{H}_{(ik)l}{}^n$ are defined in (81a) and (81c), the pair of indices (ik) indicating the projectile and the target in the specific collision integral. $C_{(ik)}$ is the corresponding constant in the cross section given by (5). Obviously $G_{(i)l}{}^n$ for any specific pair of values (l,n) must be calculated from a set of inhomogeneous linear equations.

Equation (27b), representing the distribution of energy deposited by an ion (1) in a polyatomic medium $(2,3\ldots.)$ is solved in a similar way. With the *ansatz*

$$F_{(1)\text{poly}}l^n(E) = G_{(1)}l^n E \left(\frac{E^{2m}}{N\overline{C}}\right)^n \tag{86}$$

we obtain

$$\frac{\varDelta G_{(1)}l^n}{2l+1} = G_{(1)}l^n \cdot \sum_k \alpha_k \frac{C_{(1k)}}{\overline{C}} d_{(1k)}l^n - \sum_k \alpha_k \frac{C_{(1k)}}{\overline{C}} G_{(k)}l^n \mathscr{K}_{(1k)}l^n, \tag{86a}$$

where the notation is the same as in (85a).

If the $G_{(k)}l^n$ are known from (85a) for $k = 2, 3 \ldots$, then (86a) is easy to solve recursively.

The ion *range* equation in a polyatomic target is found from (86a) by discarding the last term on the right. Substituting (81), with $\mathscr{K}_l^n = 0$, into (86a) with $\mathscr{K}_{(1k)}l^n = 0$ we obtain

$$G_{(1)}l^n = \frac{\varDelta G_{(1)}l^n}{\sum_k \alpha_k \dfrac{C_{(1k)}}{\overline{C}} \cdot \dfrac{\varDelta A_{(1k)}l^n}{A_{(1k)}l^n}}. \tag{87}$$

This equation relates the moments over the range distribution in a polyatomic target t othe moments $A_{(1k)}l^n$ over the range distribution of the ion in the constituents. In this case the most natural choice of the constant $\overline{C}$ is $\overline{C} = \sum_k \alpha_k C_{(1k)}$, but the result,

$$F_{(1)}l^n(E) = G_{(1)}l^n \left(\frac{E^{2m}}{N\overline{C}}\right)^n, \tag{87a}$$

is of course independent of the choice of $\overline{C}$.

The results of this section allow us to calculate a great variety of moments over range and damage distributions, some of which are listed in Tables I–II. The calculations were done on the CDC G-20/3100 computer system at Chalk River Nuclear Laboratories.

6. Construction of Distributions

While an infinite set of moments uniquely determines a distribution (with certain restrictions; see below) it is a rather delicate task to construct a good approximation to a distribution from a finite number of moments. Various procedures have been used in the slowing-down theory of neutrons, electrons, X-rays etc. The present approach is based on the assumption that the depth distribution of ion ranges and deposited energy is close to gaussian when the medium is random and infinite.

An alternative approach, using Chebyshev inequalities (FELLER, 1966) to obtain bounds on the integrated density, will be discussed by one of us in a subsequent paper (WINTERBON, 1970).

We follow customary usage in this field and use the term 'distribution' in the following where a statistician would say 'density'. This should not cause confusion here because we have no occasion in this work to refer to a statistician's 'distribution', which is an integrated density.

The gaussian or normal distribution is in many ways the simplest starting point. For ion ranges there appears to be experimental evidence that the gaussian is an adequate approximation, in the sense that the distribution appears to decrease like $\exp(-x^2)$ at large distances, but for deposited energy distributions there is no sufficiently accurate experimental information. There are indications from computer simulation work of PAVLOV et al. (1966) that distributions of vacancies or interstitials are close to gaussian shape, but it is felt that the number of runs made in that work is too small to permit definite statements.

Given a set of moments v_n of an unknown distribution f and an initial approximation $\psi = \psi_0$, there is a well-defined procedure for making successive approximations ψ_n to f as follows. Let the polynominals p_n be orthogonal polynominals associated with the weight function ψ. Then

$$\psi_n = \sum_{m=0}^{n} c_m p_m \psi, \tag{88}$$

where c_m is chosen so that the mth moment of ψ_m ($m \leq n$) is equal to v_m. The p_m are orthogonal polynominals so the value of c_m does not depend on n.

This procedure has the disadvantage that the approximants ψ_n are not necessarily everywhere positive. In fact if the interval is $(-\infty, +\infty)$, as it is here, then each odd approximant is negative for sufficiently large (absolute) values of the argument in one direction or the other.

If ψ_0 is a gaussian, the polynominals p_m are Hermite polynomials, and the approximants are partial sums of an Hermite polynomial series. If ψ_0 has the same mean and variance as f, we deal with a Gram-Charlier series. If the terms of the Gram-Charlier series are rearranged in a certain way, we obtain an Edgeworth series. (See, for example, CRAMER, 1945; FELLER, 1966; KENDALL & STUART, 1958).

BAROODY (1965) used Edgeworth's expansion to approximate range distributions. SANDERS (1968a, 1968b) used the same procedure, and SIGMUND (1968, 1969a) applied it to distributions of deposited energy. PRINGLE (1968), by analyzing accurate experimental range distributions, found that the best gaussian fit to his distributions was not necessarily centered around the average projected range, nor was the width of it the same as the straggling. Similar observations were made with calculated distribu-

tions in the present work. Hence it was decided to examine various other methods for determining the parameters of the gaussian. These are described in this section. Also we consider a class of series with a non-gaussian $\psi_0 \sim \exp(-\lambda|x - a|^\beta)$.

At present, we deal exclusively with planar geometry. From (43), (36), and (76) we have

$$\langle x^n \rangle = \frac{1}{E} \sum_{l=0}^{\infty} (2l + 1) F_l^n(E) P_l(\eta) = \left(\frac{E^{2m}}{NC}\right)^n \sum_l (2l + 1) A_l^n P_l(\eta), \quad (89)$$

for $M_1 = M_2$, and

$$\langle x^n \rangle = \left(\frac{E^{2m}}{NC_{(1)}}\right)^n \sum_l (2l + 1) A_{(1)l}^n P_l(\eta) \quad (89\,a)$$

for $M_1 \neq M_2$. Eq. (89a) and the last part of (89) hold for both range and damage distributions, with different values for the A_l^n and $A_{(1)l}^n$. Similar relations hold for polyatomic targets. Hence, for any value of $\eta = \cos\theta$, θ being the angle of the beam with the direction in which the depth distributions are measured, we obtain a set of averages $\langle x^n \rangle$ over these depth distributions. We define

$$\langle x^n \rangle = \nu_n \left(\frac{E^{2m}}{NC}\right)^n . \quad (90)$$

so that ν_n is dimensionless. C stands for either C, $C_{(1)}$, or $\overline{C}$, depending on the specific problem. Thus the distribution functions depend on energy only in the length unit, E^{2m}/NC. This, again, is a specific feature of power cross sections, for $W = U = 0$. When reconstructing $F(x)$ in the following, x will also have units of E^{2m}/NC.

Introducing the new variable

$$\xi = \alpha(x - a), \quad (91)$$

where a and α are not yet specified, we can write

$$F(x) = F(x(\xi)) = f(\xi) = \psi(\xi) \sum_{m=0}^{\infty} c_m \operatorname{He}_m(\xi) \quad (92)$$

where

$$\psi(\xi) = (2\pi)^{-1/2} \exp(-\xi^2/2) \quad (92\,a)$$

and $\operatorname{He}_m(\xi)$ are Hermite polynominals (ABRAMOWITZ & STEGUN, 1964).

A word should be said about convergence. The set of moments need not define the distribution uniquely (see for example, FELLER, 1966): the moments must satisfy certain restrictions in the rate of growth for there to be uniqueness. From the footnote in FELLER, p. 224, it can be seen that if the density is $0(\exp(-\lambda|x|))$ for some $\lambda > 0$, then it is uniquely determined by its moments. Since the mere existence of the moments suffices for the convergence (in the mean) of the Hermite series, and since $F(x)$ is expected to be continuous, it follows that if $F(x) = 0(\exp(-\lambda|x|))$ then the series in (92) converges to F. We expect $F(x) = 0(\exp(-\lambda x^2))$, so we assume convergence of (92). Since we have been unable to obtain asymptotic limits on the ν_n, we can of course not prove either convergence or the stronger estimate $F(x) = 0(\exp(-\lambda x^2))$.

An expression for the c_m in terms of the ν_r is derived in Appendix B, eq. B6,

$$c_m = \frac{\alpha}{m!} \sum_{r=0}^{m} \binom{m}{r} \alpha^r \nu_r \operatorname{He}_{m-r}(-a\alpha) \qquad (93)$$

For the Gram-Charlier or Edgeworth series the parameters a and α are chosen so that

$$c_1 = c_2 = 0, \qquad (94)$$

whence

$$a = \nu_1, \quad \alpha = (\nu_2 - a^2)^{-1/2}. \qquad (94\,a)$$

To try to improve apparent convergence, higher order moments were used in determining a and α. The first method tried used second and third or third and fourth moments. Thus we require

$$c_2 = c_3 = 0 \qquad (95)$$

or

$$c_3 = c_4 = 0. \qquad (95\,a)$$

Appropriate values of a and α in terms of the ν_r are given in Appendix B. Such a procedure could in principle be continued indefinitely, but the amount of labour required increases rapidly. *In these two cases we could consider ψ_0 to be a gaussian times a linear or quadratic polynomial,* so we call them "linear" and "quadratic" fits.

Another possible fitting criterion is that the c_n should decrease rapidly. This may be satisfied by minimizing

$$c_0^{-2} \sum_{n=0}^{N} c_n^2 \omega_n,$$

with the weight ω_n a rapidly increasing function of n. We have used $\omega_n = n!$ and $(n!)^2$, and got apparently good results, but have not investigated this procedure fully.

Besides the gaussian base, some fits were tried with a more general form,

$$\psi_0 = N' \exp(-\lambda |\xi|^\beta). \tag{96}$$

Only one class of fit was tried, that with

$$c_1 = c_2 = c_4 = 0 \tag{96a}$$

(ψ_0 is symmetric in ξ, so it is not possible in general to make $c_1 = c_3 = 0$). Details are reported in Appendix B.

7. Results & Discussion

Table III and Figures 5–7 show up to fourth order moments of the damage and range distributions for the case of the point source, where the distribution is considered both parallel (X) and perpendicular (Y, Z) to the initial velocity $\vec{v}$. As a length unit we use either the quantity $E^{2m}/NC_{(1)}$ or the average path length in the LSS approximation, $R(E)$, as given by eq. (15). The latter length unit is convenient for comparison with those calculations of LINDHARD et al. (1963b) that are based on the accurate Thomas-Fermi cross section. Note that all but first-order moments are given in *relative* units so that the dependence on ion energy is eliminated for $n \geq 2$.

Table III contains results for the case $M_1 = M_2$ for several values of the exponent m in the cross section. This table shows how sensitive the distributions are to the choice of the differential scattering cross section. Table IIIa indicates that for the damage distribution there are no large variations with m over the most important range, $m = \frac{2}{3}, \frac{1}{2}, \frac{1}{3}$ and $\frac{1}{4}$, except that the distribution broadens in the Y, Z plane with decreasing m (decreasing energy), as seen in $\langle \varrho^2 \rangle / \langle X \rangle^2$, and that the skewness in the X direction, as measured by $\langle \Delta X^3 \rangle / \langle \Delta X^2 \rangle^{3/2}$ has a maximum for $m \sim \frac{1}{3}$. The average damage depth $\langle X \rangle$ is always smaller than the path length R of the ion. Table IIIb shows similar results for the range distribution. Note that both ratios $\langle X \rangle / R$ and $\langle \Delta X^2 \rangle / \langle X \rangle^2$ are slightly more sensitive to changes in m than they are for the damage distributions.

For $M_1 \neq M_2$ we consider only the most important cases, $m = \frac{1}{2}$ and $m = \frac{1}{3}$. Fig. 5 shows the various first and second moments as functions of mass ratio $\mu = M_2/M_1$. For $\mu \gtrsim \frac{1}{2}$ the results appear to be insensitive to m. This is also true for higher moments (Figs. 6 & 7). The ratio $\langle X \rangle / R$ decreases with increasing μ, since for $M_1 \ll M_2$ ions undergo many large-

TABLE III. Moments over the damage and range distribution, $M_1 = M_2$. X = direction of initial velocity; Y, Z = directions perpendicular to initial velocity; $\varrho^2 = Y^2 + Z^2$; R = path length = $\int\limits_0^E dE/NS_n(E)$.

(IIIa) Damage.

m	2/3	1/2	1/3	1/4	1/8	1/16
$\langle X \rangle / \left(\dfrac{E^{2m}}{NC} \right)$	0.1560	0.2949	0.5054	0.6563	0.9922	1.251
$\langle X \rangle / R$	0.6239	0.5899	0.5054	0.4375	0.2835	0.1668
$\langle \Delta X^2 \rangle / \langle X \rangle^2$	0.3388	0.3807	0.4070	0.4286	0.5766	0.9989
$\langle \varrho^2 \rangle / \langle X \rangle^2$	0.2601	0.3146	0.4397	0.5714	1.098	2.121
$\langle \Delta X^3 \rangle / \langle \Delta X^2 \rangle^{3/2}$	0.4930	0.7333	0.8468	0.8263	0.5412	0.2260
$\langle X\varrho^2 \rangle / (\langle X \rangle \langle \varrho^2 \rangle)$	1.394	1.406	1.332	1.261	1.119	1.041
$\langle \Delta X^4 \rangle / \langle \Delta X^2 \rangle^2$	2.807	3.373	3.782	3.853	3.623	3.310
$\langle X^2\varrho^2 \rangle / (\langle X^2 \rangle \langle \varrho^2 \rangle)$	1.663	1.723	1.608	1.485	1.234	1.096
$\langle \varrho^4 \rangle / \langle \varrho^2 \rangle^2$	3.706	3.773	3.402	3.073	2.478	2.186

(IIIb) Range.

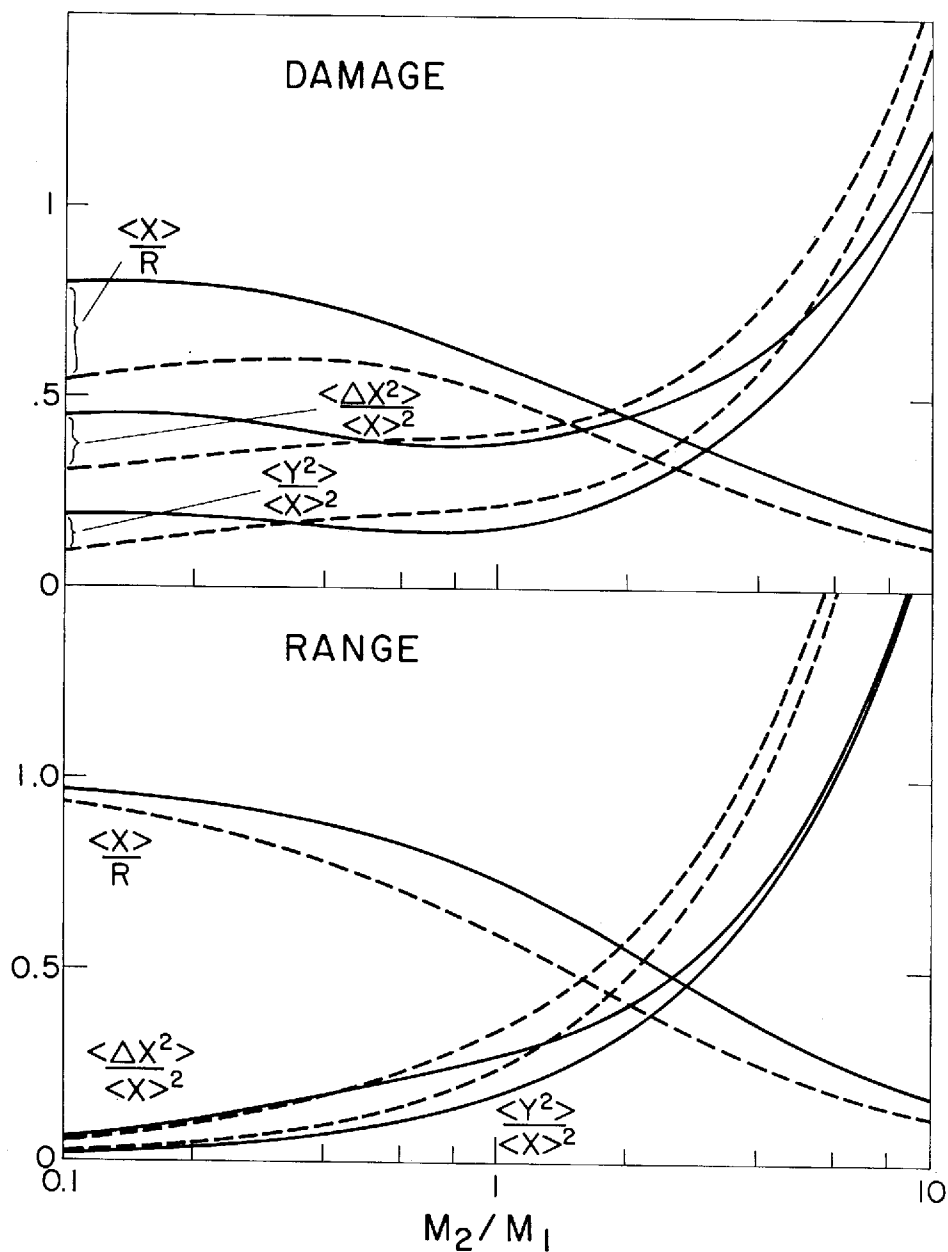| m	2/3	1/2	1/3	1/4	1/8	1/16
$\langle X \rangle / \left(\dfrac{E^{2m}}{NC} \right)$	0.2040	0.3687	0.5973	0.7500	1.069	1.301
$\langle X \rangle / R$	0.8159	0.7374	0.5973	0.5000	0.3053	0.1734
$\langle \Delta X^2 \rangle / \langle X \rangle^2$	0.2050	0.2756	0.3405	0.3846	0.5682	1.007
$\langle \varrho^2 \rangle / \langle X \rangle^2$	0.2895	0.3519	0.4825	0.6154	1.1410	2.163
$\langle \Delta X^3 \rangle / \langle \Delta X^2 \rangle^{3/2}$	0.2602	0.5456	0.6868	0.6800	0.4522	0.1962
$\langle X\varrho^2 \rangle / (\langle X \rangle \langle \varrho^2 \rangle)$	1.134	1.195	1.196	1.168	1.086	1.031
$\langle \Delta X^4 \rangle / \langle \Delta X^2 \rangle^2$	2.733	3.134	3.503	3.597	3.486	3.258
$\langle X^2\varrho^2 \rangle / (\langle X^2 \rangle \langle \varrho^2 \rangle)$	1.219	1.341	1.357	1.313	1.173	1.076
$\langle \varrho^4 \rangle / \langle \varrho^2 \rangle^2$	2.480	2.729	2.742	2.638	2.338	2.144

Fig. 5. First and second order averages over damage and range distribution as functions of mass ratio M_2/M_1; R = path length = $\int_0^E dE/(NS_n(E))$; X-direction parallel to initial velocity; $\Delta X = X - \langle X \rangle$.   Dashed line, $m = 1/3$; solid line $m = 1/2$.
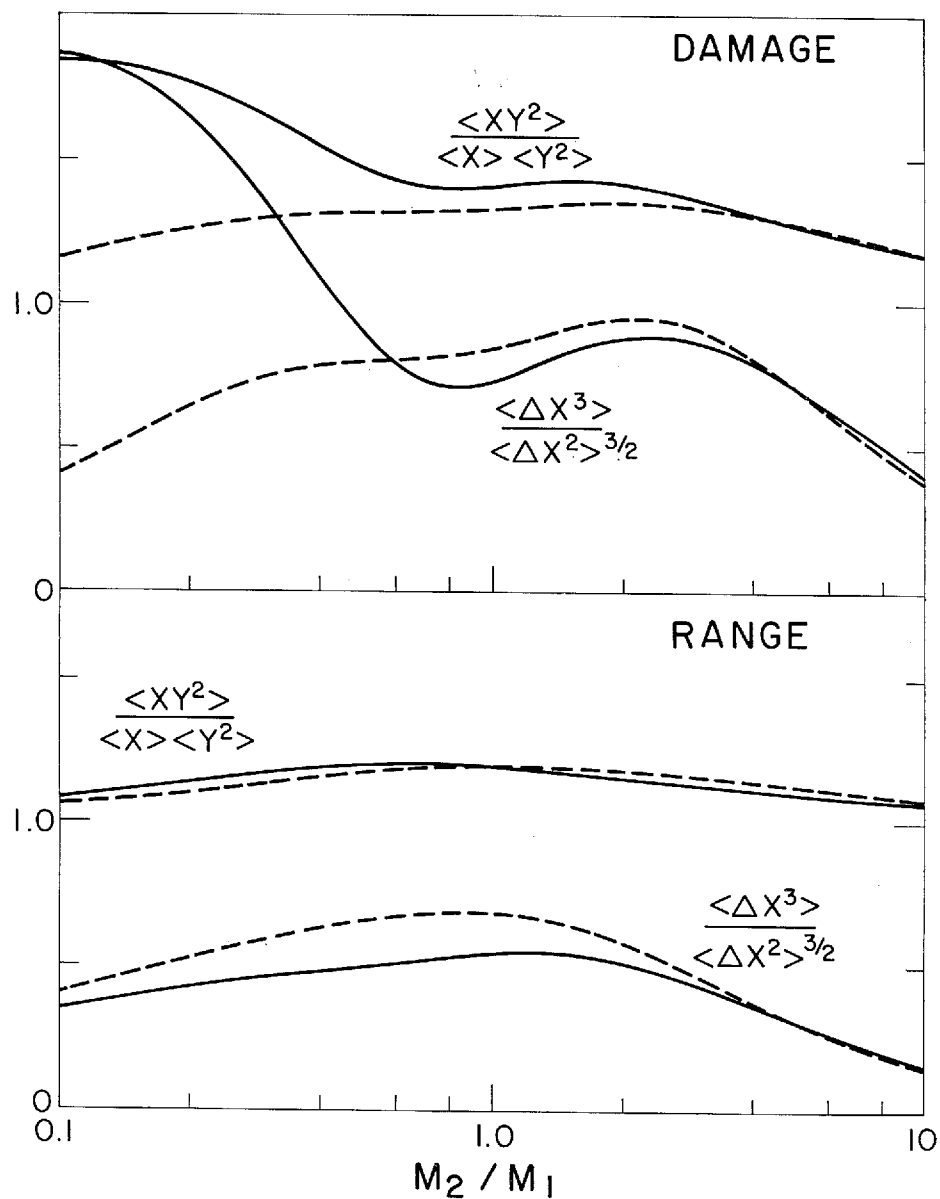
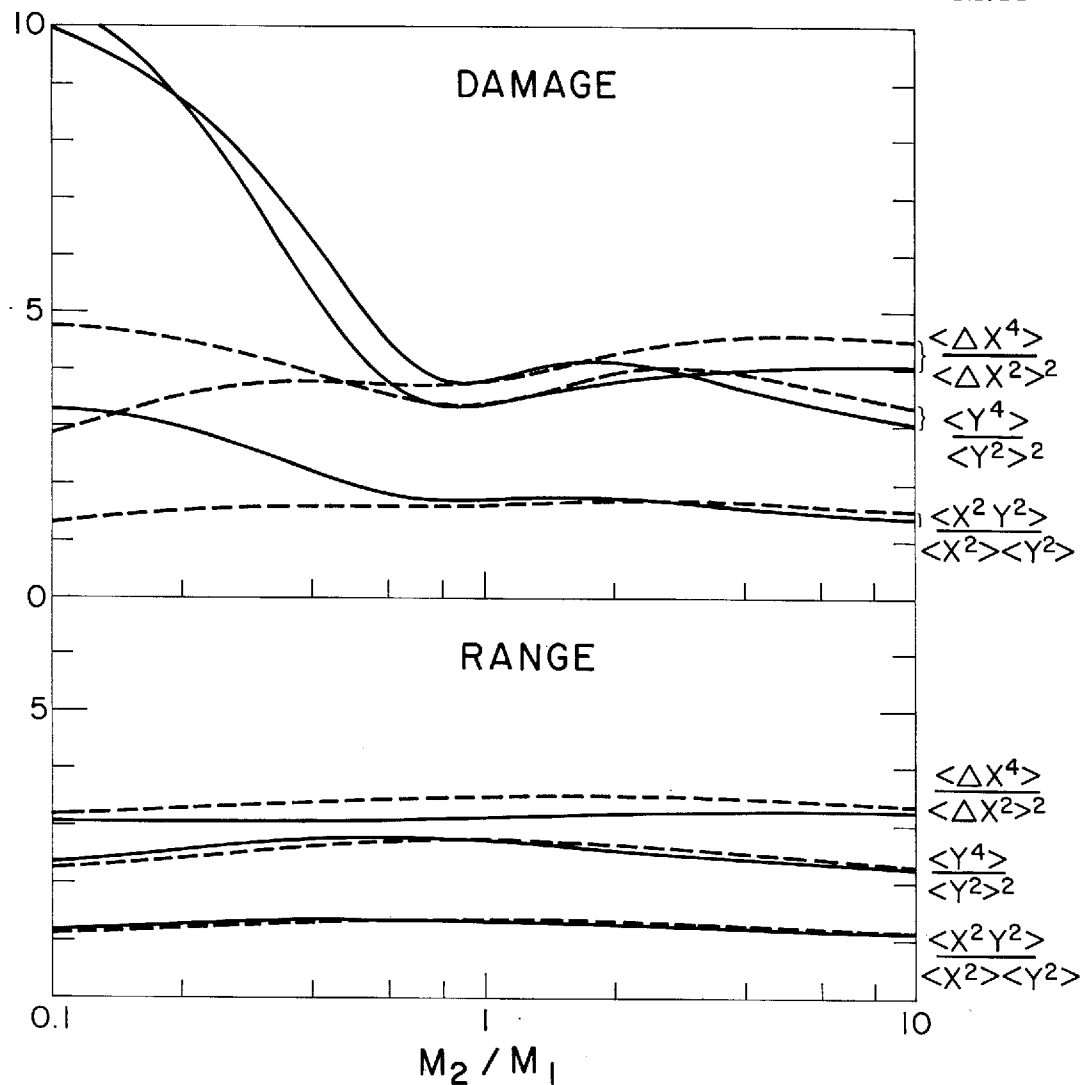Fig. 6. Third order averages over damage and range distribution. Definitions as in Fig. 5.

Fig. 7. Fourth order averages over damage and range distributions. Definitions as in Fig. 5.

angle deflections. Similarly, the distributions broaden in each dimension when μ increases.

The distributions are slightly prolate at all mass ratios considered, most pronouncedly so for $\mu < 1$. For $\mu \gg 1$ the distributions are practically spherical.

The simple stopping vs. path length argument of (18, 19) gives $\langle X \rangle / R = 0.5$ and 0.4, and $\langle \Delta X^2 \rangle / \langle X \rangle^2 = 0.333$ and 0.429, for $m = \frac{1}{2}$ and $\frac{1}{3}$ respectively. Comparison with Fig. 5 shows that this approach gives rather poor results at all mass ratios.

Figure 6 shows third order moments. For a purely gaussian distribution the ratio $\langle \Delta X^3 \rangle / \langle \Delta X^2 \rangle^{3/2}$ would be zero and $\langle XY^2 \rangle / (\langle X \rangle \langle Y^2 \rangle) = 1$. The range distribution appears to be more nearly gaussian than the damage distribution, especially for $\mu \lesssim 1$. The same conclusion can be drawn from an inspection of fourth order moments, Fig. 7. For a gaussian, one would obtain $\langle \Delta X^4 \rangle / \langle \Delta X^2 \rangle^2 = \langle Y^4 \rangle / \langle Y^2 \rangle^2 = 3$, and $\langle X^2 Y^2 \rangle / (\langle X^2 \rangle \langle Y^2 \rangle) = 1$. The most pronounced deviations from these relations occur in the damage density for $\mu \ll 1$ and $m = \frac{1}{2}$.

In Figs. 8a–c we compare range moments with the corresponding damage moments. Fig. 8a shows that the mean damage depth is consistently smaller than the mean projected range. The difference is small except for $\mu \ll 1$ and $m = \frac{1}{3}$ where it is a factor of ~ 2. In this case heavy damage is created all over the ion path, so that despite energy transport of recoiling atoms the ion comes to rest essentially at the far end of the damage cloud, while $\langle X \rangle$ is in the center. This picture is consistent with Fig. 8b that shows that the damage distribution is much broader than the range distribution for $\mu \ll 1$. It may be surprising to see that the opposite is true for $\mu \gtrsim 1$. This is obviously because we are considering the damage distribution of *many events*. For $\mu \gtrsim 1$, the ion undergoes large deflections, but mainly those in the beginning, where the ion still has much energy to share with its collision partners, determine the region where the energy is located, while those collisions undergone by the ion toward the end of its slowing down still may contribute to range straggling, but not to a broadening of the damage distribution. Note that the effect is not very pronounced, about a factor of 1.3 in the linear dimensions at the highest mass ratios considered. Fig. 8c shows the same qualitative effect for the transverse extension $\langle Y^2 \rangle$, except that $\langle Y^2 \rangle_R / \langle Y^2 \rangle_D$ goes through a maximum near $\mu = 2$.

Some approximate damage and range distributions are plotted in Figs. 9–11. Fig. 9 (damage, $m = \frac{1}{3}$, $\mu = 1$) compares various methods of fitting. Case 1 is the Edgeworth expansion, cases 2 and 3 the linear and quadratic fits, and case 4 the non-gaussian. (In this case the exponent $\beta = 1.49$). For the Edgeworth and non-gaussian cases the heavy line is ψ_0, the initial approximation. In the other two it includes the linear or quadratic polynomial as well. The two to four lightly drawn lines include the first correction terms. The Gram-Charlier expansion is not shown. In it the density
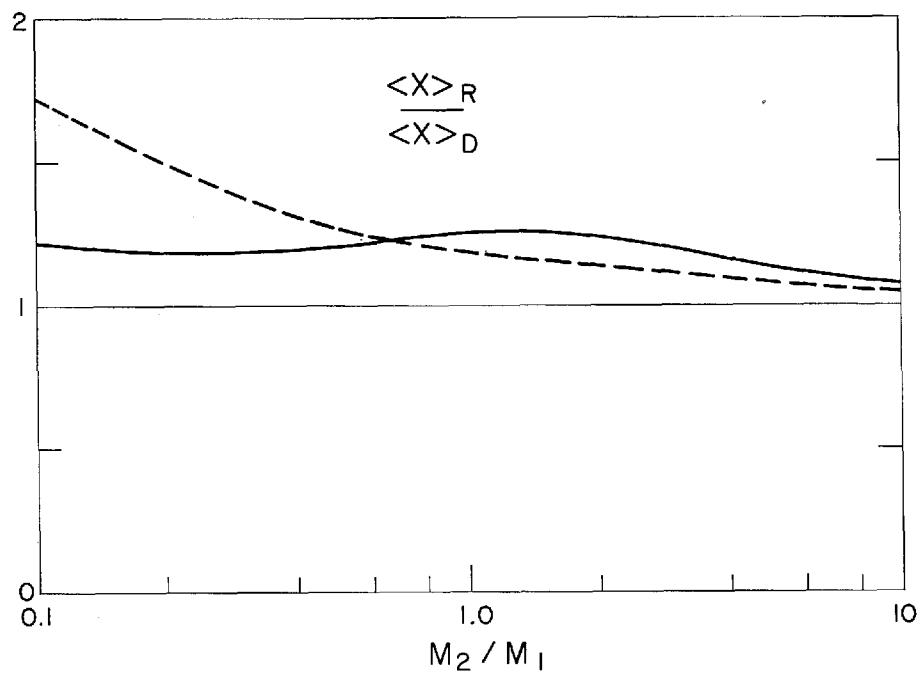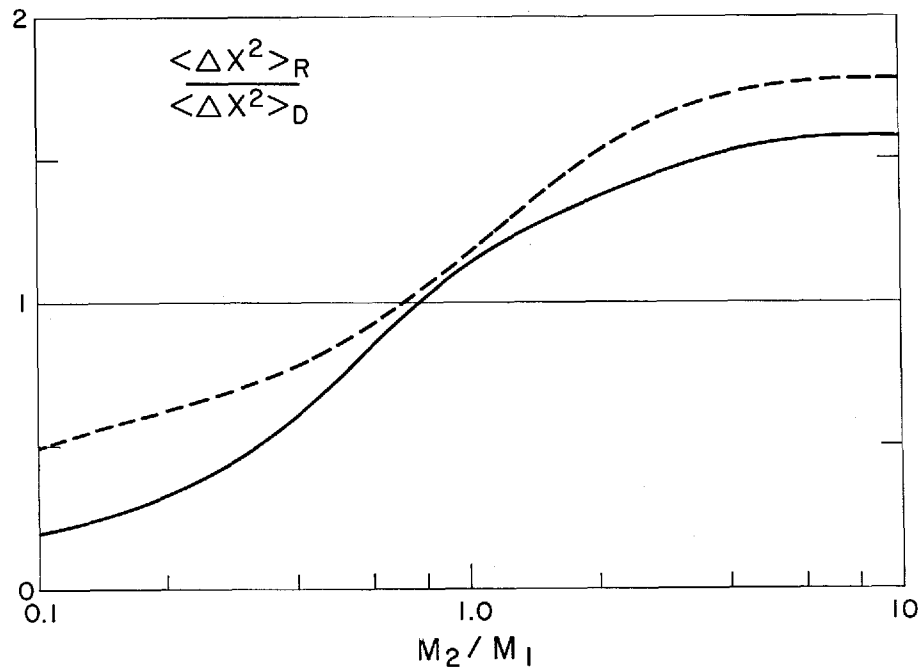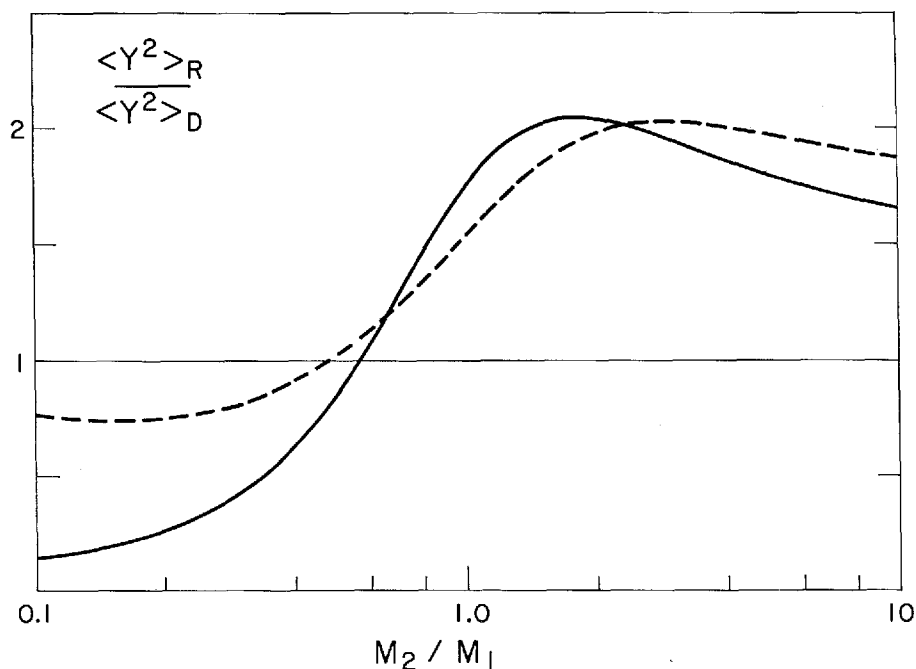
Fig. 8a.

Fig. 8b.

Fig. 8 c.

Fig. 8. Ratio between averages over range and damage distributions as a function of mass ratio. Dashed line, $m = 1/3$; Solid line, $m = 1/2$.

a) First order averages. $\langle X \rangle_R$ = average projected range; $\langle X \rangle_D$ = average damage depth.
b) Second order averages. $\langle \Delta X^2 \rangle_R$ = straggling of projected range; $\langle \Delta X^2 \rangle_D$ = width of the damage depth distribution.
c) Second order averages. $\langle Y^2 \rangle_R$ = transverse straggling of range distribution; $\langle Y^2 \rangle_D$ = transverse width of damage distribution.

had pronounced oscillations, indicating that the fit was poor. In the Edgeworth expansion the minimum outside the surface deepens and approaches the surface as the order of approximation increases, and the tail within the target is not well fitted. In the linear and quadratic fits the tail does not appear to change with the order of approximation and the minimum outside the surface is farther out. Again this minimum moves in with increasing order. The non-gaussian curve, case 4, has a narrower peak because with $\beta = 1.49$, the tails have greater weight.

Range distributions were all fitted well with the Edgeworth expansion, and the exponents β of case 4 were close to 2.

Figure 10 compares damage and range distributions ($m = \frac{1}{2}$). The Edgeworth expansion for damage in 10a ($\mu = 4$) converges reasonably
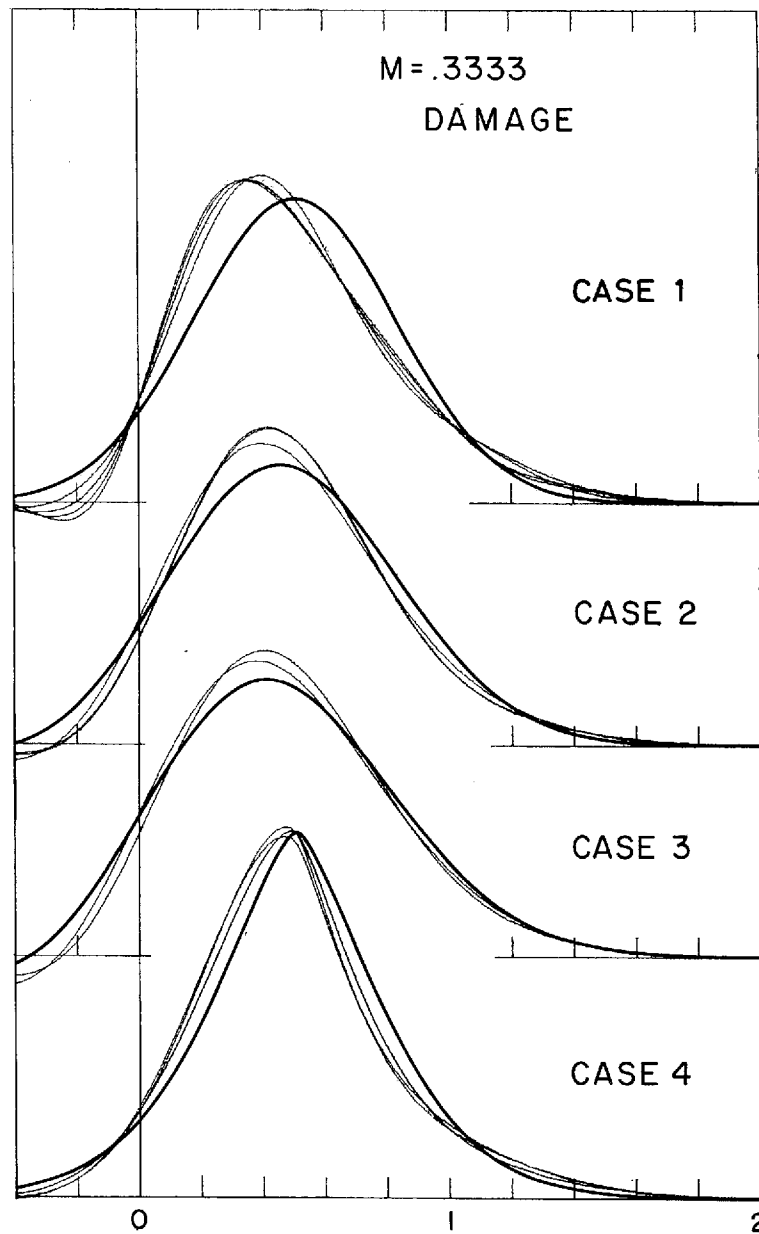
4*

Fig. 9. Damage distribution as a function of depth. In units of $R(E)$. $m = \frac{1}{3}$, $\mu = 1$. Heavy line, initial approximation Light lines, higher approximations.

1) Edgeworth series.
2) $\psi_0 =$ Gaussian times linear function.
3) $\psi_0 =$ Gaussian times quadratic.
4) Non-gaussian, $\psi_0 = N' \exp(-\lambda |\xi|^\beta)$, $\beta = 1.49$.

well; for $\mu = \frac{1}{4}$ (Fig. 10 b) the Edgeworth expansion gave no signs of convergence. The gaussian parameters plotted here were obtained by minimizing

$$c_0^{-2} \sum_{n=0}^{20} c_n^2 (n!)^2.$$

Approximants ψ_0 (the heavy line), ψ_1, ψ_2, and ψ_{20} are plotted.

Figure 11 shows isodensity contours (contour interval 10% of max-. imum density) in the $X-Y$ plane of range and damage for $m = \frac{1}{2}$, $\mu = 1$, The distributions were constructed using the formalism of Appendix C with parameters chosen to minimize

$$c_{00}^{-2} \left(\sum_{m=0}^{20} c_{m0}^2 (m!)^2 + \sum_{n=0}^{10} c_{0n}^2 (2n)! \right).$$

At high densities both distribution functions narrow toward the rear, but at low densities they appear to broaden. The maximum of both distributions occurs closer to the surface than the maximum of the corresponding depth distributions, especially in case of the range plot. This is consistent with increasing lateral spread with increasing depth, as evident from fig. 11.

8. Comparison with Experiment & Computer Simulation

Radiation Damage Measurements

In a previous communication (SIGMUND & SANDERS, 1967) we attempted to compare some results of the theory with experimental radiation damage distributions. Sufficient evidence was found to support one of the main results of the theory, namely that the average damage depth does not differ very much from the average projected ion range (Fig. 8 a). There are as yet few experimental results on damage distributions*, and several problems occur when these are compared with theory.

a) Some experimental techniques, such as those based on the orientation dependence of Rutherford scattering (BØGH, 1968), the change in optical reflection (HINES et al., 1960), and the dependence of the sputtering yield on prebombardment (MacDONALD et al., 1966 a, b) can be used only on single crystals. Therefore low-dose bombardment may lead to damage distributions that are more or less influenced by channeling effects. High-dose bombardment, on the other hand, leads to saturation effects of bombardment damage and, in some cases, the distributions

* Note added in proof: Substantial progress has been made since the submission of this paper. The reader is referred to the Proceedings of an Int. Conf. on Ion Implantation in Semiconductors, Thousand Oaks, Calif., 1970, to be published in Radiation Effects.
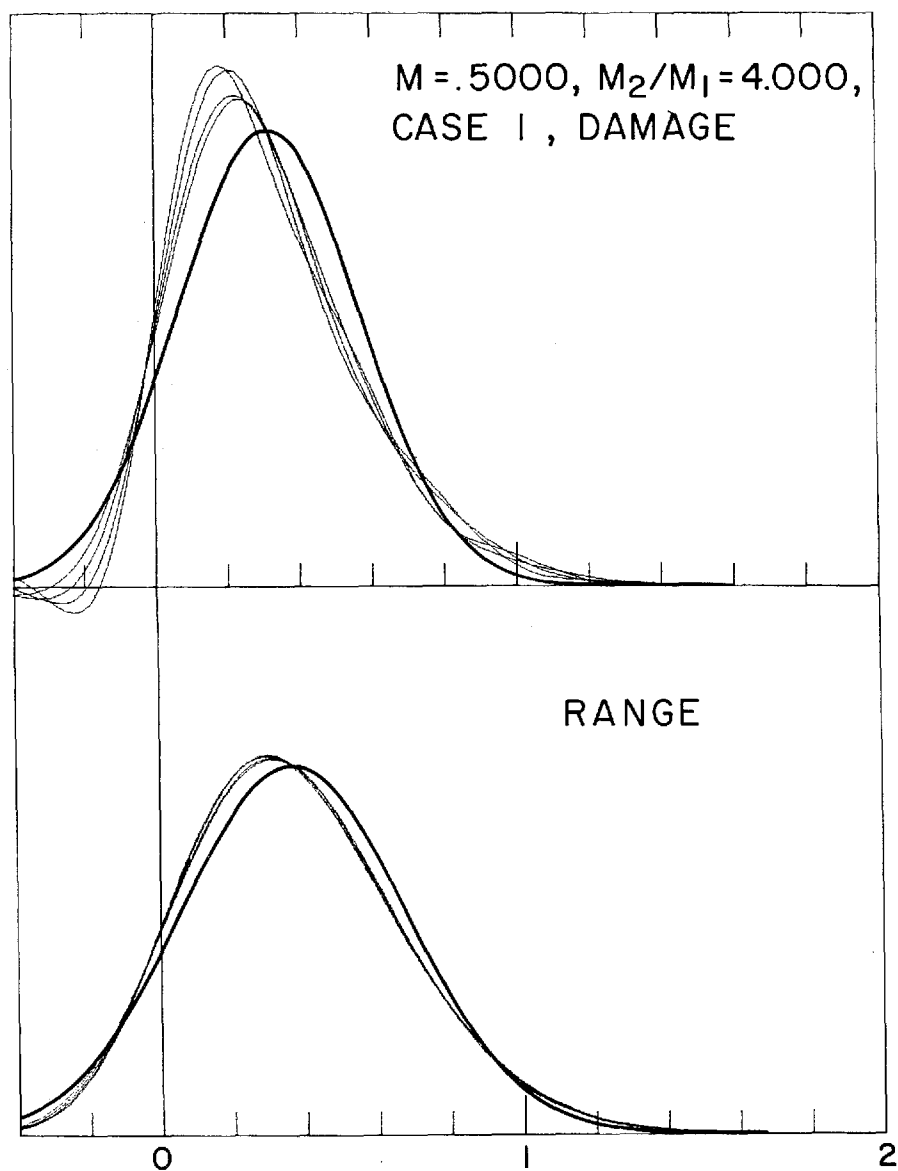
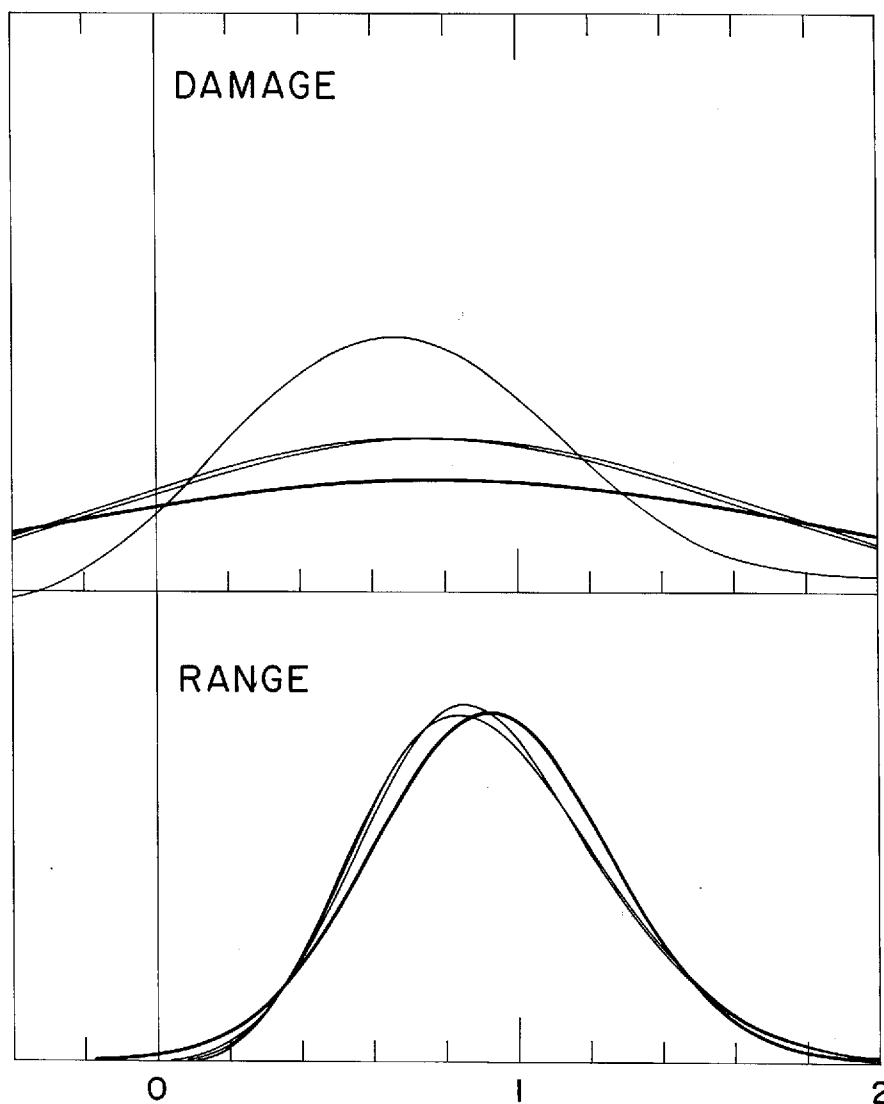Fig. 10a.

M = .5000, $M_2/M_1 = \frac{1}{4}$, CASE I

Fig. 10b.

Fig. 10. Damage and Range Distributions. Depth in units of $R(E)$. $m = \frac{1}{2}$. Heavy line, initial approximation. Edgeworth series, except 10b, damage

Gaussian parameters for damage density in Fig. 10b chosen by minimizing weighted sum of squares of the c_n. Base density ψ_0, ψ_1, ψ_2 and ψ_{20} shown.
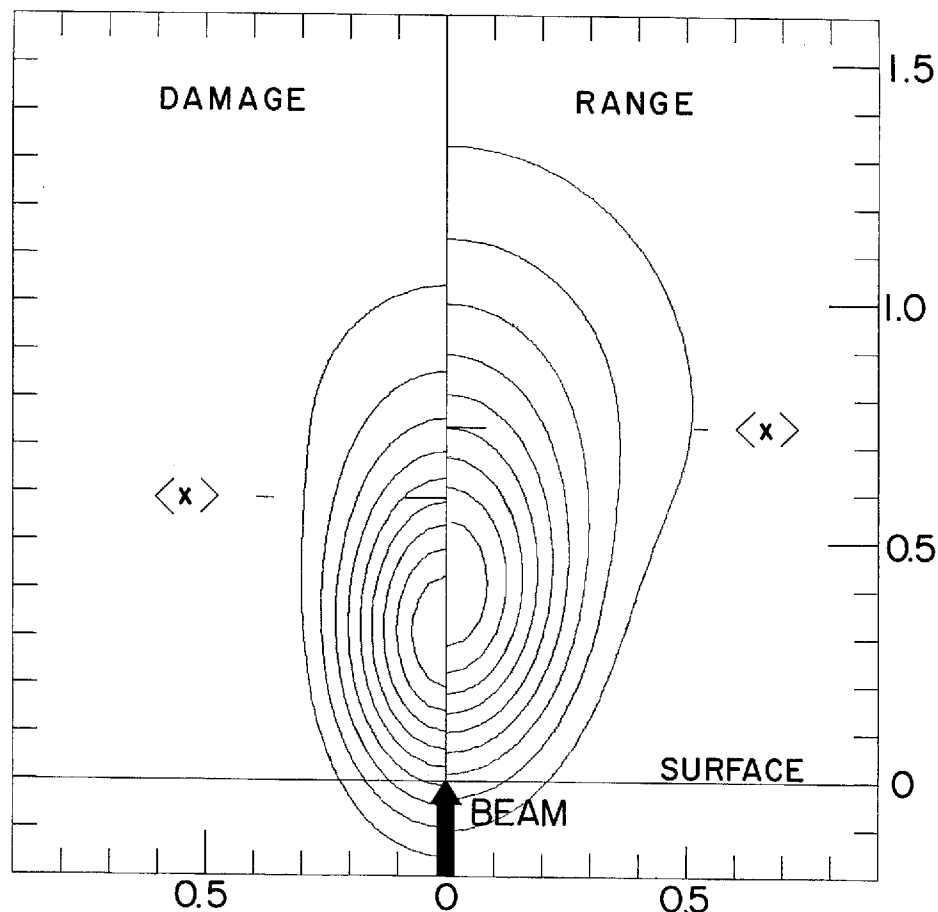
Fig. 11. Damage and Range isodensity Contours. $m = \frac{1}{2}$, $\mu = 1$. Contour interval 10% of maximum. Length in units of $R(E)$.

might change because of radiation-enhanced diffusion. Therefore experiments on single crystals can be used for quantitative comparison only when done at sufficiently low doses to prevent saturation effects and when the ion beam has not been aligned with a channeling direction.

b) Physical properties that are affected by ion bombardment damage may also be affected by implanted ions. The distinction between the ion range and damage distributions appears most direct with the orientation dependence of Rutherford scattering (DAVIES et al., 1967).

c) Electron microscopy of large defects (PARSONS et al., 1964; MERKLE, 1966; THOMAS et al., 1969) leads to results that are not necessarily comparable with the present theory. First, not all deposited energy leads to visible damage. There may be a threshold energy for creating visible damage clusters, the value of which is probably in the keV region but is not accurately known (MERKLE, 1966; THOMAS et al., 1969; HÖGBERG et al., 1969 a, b). Consequently, the region where visible damage is created need not coincide with the actually damaged region. Second, even when polycrystalline samples are irradiated the part of the target that is investigated under the microscope is often a crystallite of definite (low index) orientation, so that channeling may play a role. Third, image-size distributions of damage clusters, which are measured more easily than depth distributions (PARSONS et al., 1964; THOMAS et al., 1969), are not comparable to the quantities discussed in the present paper, since they concern properties of *single* collision cascades.*

With these reservations in mind, we find that none of the existing experimental data can be used for quantitative comparison with our theory. However, depth distribution measurements by use of Rutherford scattering are being performed currently by several groups.** For a more qualitative comparison, we discuss the work of HINES et al. (1960); MACDONALD et al. (1966 a, b), and NORRIS (1969).

HINES et al. bombarded quartz, with keV heavy rare gas ions at doses around 10^{14} ions/cm^2. The effective thickness of the damaged layer was determined from optical reflexion measurements and turned out to be largely independent of ion dose. One would expect, therefore, that neither saturation effects nor diffusion played a significant role. Table IV shows experimental results and several calculated range and damage quantities. The effective layer depth can be estimated from the sum $\{\langle x \rangle + a \langle \Delta x^2 \rangle^{1/2}\}_{\text{damage}}$, where a is a number of the order of 1 to 2. There is good agreement between measured and calculated depths for Ne$^+$ and A$^+$ bombardment, while the calculated depths are much smaller than the measured ones for Kr$^+$ and Xe$^+$ bombardment. This discrepancy is probably caused by channeling of

* Note added in proof: Average cluster size is discussed in a forthcoming paper by J. E. WESTMORELAND & P. SIGMUND (Radiation Effects, 1970).

** Note added in proof. In three recent papers on damage-depth distributions measured by Rutherford-scattering, comparison is made with results of the present paper (E. BØGH, P. HØGILD, & I. STENSGAARD, Rad. Eff. 1970; L. C. FELDMAN & J. W. RODGERS, J. Appl. Phys. 1970; F. H. EISEN, B. WELCH, J. E. WESTMORELAND, & J. W. MAYER; Atomic Collision Phenomena in Solids (ed. by D. W. PALMER et al.) North Holland 1970 p. 111). We also refer to a forthcoming paper on depth distributions in the electronic-stopping region by P. SIGMUND, M. T. MATTHIES, & D. L. PHILLIPS.

TABLE IV. Range and Damage Quantities for Quartz Bombarded with Rare Gas Ions. Measured Layer Depth from Measurements of HINES and ARNDT (1960). In the calculations, SiO_2 has been approximated by a monatomic target with the same density, atomic number 10 and atomic weight 20.

Ion	E	ε	$\langle X \rangle$ Damage	$\langle \Delta X^2 \rangle^{1/2}$ Damage	$\langle X \rangle$ Range	$\langle \Delta X^2 \rangle^{1/2}$ Range	Measured Layer Depth
	keV		Å	Å	Å	Å	Å
Ne+	38.3	1.14	372	229	450	236	740
($m = 1/2$)	43.9	1.31	428	264	518	272	850
	51.8	1.55	504	310	610	320	950
A+	22.9	0.422	215	150	259	114	600
($m = 1/2$)	38.4	0.706	360	251	434	191	700
	59.0	1.087	554	386	666	293	1000
Kr+	20.3	0.094	84	50	123	41	500
($m = 1/3$)	39.7	0.183	131	78	193	64	600
	59.0	0.272	171	101	251	83	670
Xe+	20.3	0.039	75	43	119	32	470
($m = 1/3$)	39.4	0.075	117	67	185	50	530
	59.0	0.113	154	88	243	65	580

the ions. Note, however, that in pure silicon a dose of 10^{14} Xe+ ions would be sufficient to suppress channeling almost completely (DAVIES et al., 1964).

MACDONALD et al. (1964 a, b) measured the sputtering yield of germanium for low energy A+ ions (100–200 eV) as a function of the sputtered layer thickness. The targets were pre-bombarded with 500–1000 eV rare gas ions, and the sputtering yield was enhanced over the layer thicknesses that corresponded to the penetration depths of the pre-bombarded ions. Typical pre-bombardment doses were 10^{16} to 10^{17} ions/cm², enough to make the target surface amorphous (PARSONS, 1965; MAYER et al., 1968). Also, with a range of about 20 Å the (calculated) dopant concentration is of the order of 1 dopant ion/atom within the penetration depth and, finally, the layer thickness sputtered by the pre-bombardment may well be greater than the range of the ions. All these factors indicate that the measurements can provide only a very rough estimate of the damage and penetration depth of the pre-bombarded ions, and the good agreement with the calculated depths (SIGMUND et al., 1967) confirms this. A distinction between range and damage distributions does not appear feasible.

NORRIS (1969) measured depth distributions of vacancy clusters observed by stereo electron microscopy in gold and nickel bombarded with 80 to

150 keV gold and mercury ions at doses of the order of 10^{15} ions/cm². Channeling of the ions plays a role but does not appear to be dominant, at least not in the target of (112) orientation. The results were compared to measured and calculated ion range distributions (for random slowing down) and it was found that the average depth of vacancy clusters was smaller than one would expect from our Fig. 7 a. The difference is not very pronounced, possibly still within the experimental accuracy. Note that less than one cluster is observed per incident ion, and that the average cluster diameter is of the order of the average damage depth.

A similar investigation has been carried out by THOMAS et al. (1969) at lower ion energies (5 to 40 keV) and much smaller ion doses (10^9 to 10^{12} ions/cm²). The measured depth distributions appear to be dominated by channeling and dechanneling of the bombarding ions. A comparison with these results is, therefore, outside the scope of this paper.

Range Measurements

Although a considerable amount of information on range distributions is contained in Tables I–III we do not make a comparison with measured range distributions in this paper. There are several reasons for this. First, ion ranges are not a main subject of this paper. Second, it has been well documented that random-slowing-down theory with the Thomas-Fermi cross section predicts ion ranges accurately (LINDHARD et al., 1963 b; SCHIØTT, 1966, 1968). Third, contrary to radiation damage distributions, range distributions can be measured very accurately (for recent reviews see MAYER & MARSH, 1969; MAYER et al., 1969), and for a quantitative comparison an accuracy of at least 10% in calculated average range and straggling is required. Fig. 4 b shows that the difference between the two representative cases $m = \frac{1}{2}$ and $\frac{1}{3}$ is usually larger than this limit and, more important, electronic stopping is usually not negligible at energies where measurements of high relative accuracy can be made. Some results, however, mainly on very heavy ions in the elastic stopping region, will be compared with experimental results elsewhere (WINTERBON, 1970).

Computer Simulation

Computer simulation has been used occasionally to calculate ion ranges and collision cascades. In the present context we are mainly concerned with Monte-Carlo-type computer codes, where collisions are governed by a cross section. These calculations are essentially equivalent to ours, provided that the cross sections are similar.

TABLE V. Comparison Between Range Quantities Found from Computer Simulation (OEN et al., 1964) and Analytic Calculation (present work).

a) Straggling in Projected Range, $\langle \Delta X^2 \rangle^{1/2} / \langle X \rangle$.

Ion-Target	M_2/M_1	Energy Range (keV)	Computed Straggling	From Fig. 5 $m = 1/2$	From Fig. 5 $m = 1/3$
Xe+ – Al	0.20	5 –250	0.25–0.30	0.33	0.30
K+ – Al	0.64	5 –100	0.42–0.47	0.47	0.50
Cu+ – Cu	1.0	1.75–250	0.47–0.54	0.52	0.59
Kr+ – W	2.16	4.5 –250	0.57–0.63	0.66	0.78

b) Transverse Spread $\langle \varrho^2 \rangle / \langle X^2 \rangle$

Ion-Target	Mass Ratio	Computed	From Fig. 5 $m = 1/2$	From Fig. 5 $m = 1/3$
Xe+ – Al	0.20	0.08	0.07	0.09
K+ – Al	0.64	0.18–0.23	0.18	0.24
Cu+ – Cu	1.0	0.28–0.34	0.27	0.36
Kr+ – W	2.16	0.50–0.56	0.48	0.65

The most extensive study of this type has been done by OEN et al. (1963, 1964), but only range distributions were investigated. It was already pointed out in these papers that *average* ranges calculated for purely elastic scattering agree well with experimental results at sufficiently low ion energies, and also with the range-energy formula of LINDHARD et al. (1963b), in those cases where good agreement is expected. Table V shows a comparison between computed *straggling* data (both longitudinal and transverse) with our analytical results. The computer data are based on Thomas-Fermi interaction with neglect of electronic stopping. Most of the computed straggling parameters depend slightly on energy, because they are not based on a power cross section. One recognizes that this variation with ion energy has about the same magnitude as the difference between our results for $m = \frac{1}{2}$ and $\frac{1}{3}$, and the general agreement is excellent. We made this comparison only to give an indication of the accuracy with which analytical and Monte-Carlo range calculations can agree with each other, provided the input parameters are in close enough agreement. Note that a slight difference is always expected, especially at low energies, since the interaction potential has to be truncated at some finite distance in a Monte-Carlo simulation of binary collision events.

Quite recently, PAVLOV et al. (1967) made a series of Monte-Carlo simulations to get both range and damage depth distributions for several ions implanted in silicon, for applications in ion-implanted semi-conductors. Ion doses were about the same (400–1000 ions for each energy and ion-target combination) as those of OEN et al. Mostly light ions were used in the medium and upper keV region, so that electronic stopping (which was taken into account) dominated. While some runs have been made simulating arsenic ions bombarding silicon, where electronic stopping is only a minor correction at $E \lesssim 50$ keV, damage distributions were not recorded in just these runs. Hence, only a qualitative comparison is possible for the $Al^+ - Si$ bombardments, where the ratio between the median ion range and the median damage depth turned out to decrease from 1.52 to 1.44 from $E = 25$ to 150 keV. This is to be compared with our calculated ratio $\langle x \rangle_R / \langle x \rangle_D = 1.25$ for $\mu \approx 1$ and $m = \frac{1}{2}$ (Fig. 8a). The difference may be caused by the difference between median and average penetration depths and/or the fact that hard-sphere scattering was assumed in the computations to simulate low-energy collisions. The difference between vacancy and interstitial distributions is considered to be insignificant (SIGMUND et al., 1968).

Backscattering of Ions

A very sensitive check on the validity of calculated range distributions is the backscattering coefficient α of the implanted ions. Preliminary calculations (SIGMUND, 1968) show that α depends very sensitively on the mass ratio μ. The results are in qualitative agreement with experimental data of BROWN et al. (1963). A joint experimental and theoretical effort to establish back-scattering coefficients for a number of ion-target combinations has been started.

Sputtering Measurements

The distribution of deposited energy is a key quantity in the theory of sputtering. First, the amount of energy deposited *outside* a target surface determines the sputtered *energy* (SIGMUND, 1968) and can be measured thermometrically (ANDERSEN, 1968). Second, the energy deposited *in* the target surface is converted into kinetic energy of a number of slowly moving atoms, part of which can get sputtered. The general formula for the sputtering yield is (SIGMUND, 1969a)

$$S(x, E, \eta) = \Lambda F(x, E, \eta), \tag{97}$$

where Λ is a material constant, x the distance between the bombarded and the sputtered surface (for backsputtering $x = 0$), E the ion energy and η the cosine of the angle of incidence of the beam. $F(x,E,\eta)$ is the deposited energy distribution for either equal or unequal masses, in the notation of eq. (38).

It was shown that eq. (97) can be used successfully to predict sputtering ratios for a great number of ion-target combinations and to obtain good agreement with experimental results. While extensive use has been made of the results of the present paper in the sputtering work, there is no need for repeating the results here.

In view of recent thermometric measurements of ANDERSEN (1968, 1970), a detailed discussion of the sputtered energy would be desirable. While several qualitative predictions of the theory (SIGMUND, 1968) were confirmed by the experiments, the quantitative agreement is satisfactory for only a limited range of mass ratios. More accurate estimates of the sputtering efficiency on the basis of the results of the present paper will be reported elsewhere (WINTERBON, 1970).

APPENDIX A

Moment Integrals

The first integral in eq. (78) in the equal mass case, has the form

$$I(a,b,l) = \int_0^1 dt\, t^{-1+a}(1-t)^{-1+b} P_l((1-t)^{1/2}) \tag{A1}$$

so that $I(a,b,0) = B(a,b)$, the beta function and $I(a,b,1) = B(a,b+\frac{1}{2})$. Using the Legendre polynominal recurrence relation we find

$$(l+1)I(a,b,l+1) = (2l+1)I(a,b+\tfrac{1}{2},l) - lI(a,b,l-1). \tag{A2}$$

To evaluate the I's from this, the beta functions $B(a,b)$ and $B(a,b+\frac{1}{2})$ are calculated, and from these the quantities $B(a,b+1)$, $B(a,b+\frac{3}{2})$, $B(a,b+2)$, ... are obtained using the recursion relation

$$B(a,b+1) = \frac{b}{a+b} B(a,b). \tag{A3}$$

In the unequal-mass case, the first integral is

$$I_\gamma(a,b,l) = \int_0^\gamma dt\, t^{-1+a}(1-t)^{-1+b} P_l((1-t)^{1/2} + \alpha t(1-t)^{-1/2}) \tag{A4}$$

Now $I_\gamma(a,b,o) = B_\gamma(a,b)$, the incomplete beta function. From the Legendre polynominal recurrence relation, and the obvious relation

$$I_\gamma(a,b,l) = I_\gamma(a,b-1,l) - I_\gamma(a+1,b-1,l), \tag{A5}$$

we find

$$\left.\begin{aligned} (l+1)I_\gamma(a,b,l+1) = (2l+1)[(1-\alpha)I_\gamma(a,b+\tfrac{1}{2},l) + \\ \alpha I_\gamma(a,b-\tfrac{1}{2},l)] - lI_\gamma(a,b,l-1). \end{aligned}\right\} \tag{A6}$$

The required values of the incomplete beta function are generated from the initial values $B_\gamma(a,b), B_\gamma(a,b+\frac{1}{2})$ with the recursion relation

$$\left.\begin{aligned} B_\gamma(a,b+1) = \gamma^a(1-\gamma)^b/(a+b) + bB_\gamma(a,b)/(a+b) \\ (b \neq 0) \end{aligned}\right\} \tag{A7}$$

(this may be derived by integration by parts and using $B_\gamma(a,b+1) = B_\gamma(a,b) - B_\gamma(a+1,b)$ and, if necessary, $B_\gamma(a,o) = \dfrac{\gamma^a}{a} F(1,a;a+1;\gamma)$, where F is the hypergeometric function.

The second integral in eq. (78) is essentially the same in both equal-mass and unequal-mass cases:

$$K_l{}^n(a) = \int_0^1 dt\, t^{a-1} P_l(t^{1/2}) = 2 \int_0^1 dx\, x^{2a-1} P_l(x).$$

(A 8)

From ERDELYI et al. (1954), p. 313, we have

$$K_l = \frac{2\pi^{1/2}\,\Gamma(2a)}{2^{2a}\,\Gamma\!\left(a + \dfrac{1-l}{2}\right)\Gamma(a+1+l/2)}.$$

(A 9)

We use the duplication formula for Γ-functions, (ABRAMOWITZ & STEGUN, 1964),

$$\Gamma(2a) = 2^{2a-1}\pi^{-1/2}\Gamma(a)\Gamma(a+\tfrac{1}{2}),$$

to get

$$K_l(a) = \frac{\Gamma(a)\,\Gamma(a+1/2)}{\Gamma\!\left(a + \dfrac{1-l}{2}\right)\Gamma(a+1+l/2)}$$

(A 10)

from which

$$K_0(a) = 1/a$$

$$K_1(a) = 1/(a + \tfrac{1}{2})$$

and

$$K_{l+2}(a) = \frac{a - (l+1)/2}{a + 1 + l/2}\, K_l(a).$$

(A 11)

APPENDIX B

Expansions of the Distributions

In this paragraph we derive the coefficients for expansion of depth distribution functions in terms of Hermite or more general orthogonal polynomials. Let the (unknown) distribution function be $F(x)$, and introduce the new variable

$$\xi = \alpha(x - a),$$

(B 1)

so we can write

$$F(x) \equiv f(\xi) = \psi(\xi) \sum_{m=0}^{\infty} c_m He_m(\xi),$$

(B 2)

where

$$\psi(\xi) = (2\pi)^{-1/2}\exp(-\xi^2/2).$$

(B 3)

We still have the freedom of choosing the parameters α and a in (B 1).

We wish to express the c_m in terms of the moments v_r of F,

$$v_r = \int_{-\infty}^{\infty} dx\, x^r F(x). \tag{B4}$$

Using the orthogonality of the Hermite polynomials we have

$$\left.\begin{aligned}
n!\,c_n &= \int d\xi\, He_n(\xi) f(\xi) \\
&= \alpha \int dx\, He_n(\alpha(x-a)) F(x) \\
&= \alpha \sum_{m=0}^{[n/2]} \frac{n!\,(-)^m \alpha^{n-2m}}{m!\,2^m (n-2m)!} \sum_{r=0}^{n-2m} \binom{n-2m}{r} (-a)^{n-2m-r} \int dx\, x^r F(x)
\end{aligned}\right\} \tag{5B}$$

The integral is v_r. Interchanging the order of summation and recognizing the inner sum as a Hermite polynomial, we have

$$c_n = \frac{\alpha}{n!} \sum_{r=0}^{n} \binom{n}{r} \alpha^r v_r\, He_{n-r}(-a\alpha). \tag{B6}$$

The conditions $c_i = 0$ reduce to the following:

c_1: $a - v_1 = 0$

c_2: $(a^2 - 2av_1 + v_2)\alpha^2 - 1 = 0$

c_3: $(a^3 - 3a^2 v_1 + 3av_2 - v_3)\alpha^2 - 3(a - v_1) = 0$

c_4: $\alpha^4(a^4 - 4a^3 v_1 + 6a^2 v_2 - 4av_3 + v_4) - 6\alpha^2(a^2 - 2av_1 + v_2) + 3 = 0.$

In the usual Gram-Charlier expansion one chooses $c_1 = c_2 = 0$ and therefore $a = v_1$ and $\alpha = b^{-1/2}$, where $b = v_2 - v_1^2$. In the $c_2 = c_3 = 0$ case,

$$a = v_1 + (d/2)^{1/3}, \quad \text{and}$$

$$\alpha^{-2} = b + (d/2)^{2/3},$$

where

$$d = v_1^3 + 3bv_1 - v_3.$$

In the $c_3 = c_4 = 0$ case,

$$\left.\begin{aligned}
a &= v_1 + (d/2)^{1/3} - z, \quad \text{and} \\
\alpha^{-2} &= b + (d/2)^{2/3} + e, \quad \text{say,}
\end{aligned}\right\} \tag{B7}$$

where

$$e = z^2((d/2)^{1/3} + z/3)/((d/2)^{1/3} + z)$$

and z is a root of

$$h(1+z)^2 - 2z^3(d/2)^{4/3}(4 + 5z + 2z^2 + z^3/3) = 0 \tag{B7a}$$

with $h = v_4 - 4v_3 v_1 - 3v_2^2 + 12v_2 v_1^2 - 6v_1^4 + 6(d/2)^{4/3}$.

There are two real roots of (B7a), only one of which is useful.

Consider now a non-gaussian distribution:

Let

$$\psi(\xi) = N' \exp(-\lambda|\xi|^\beta).$$ (B8)

The moments of ψ are ($\nu = (2n+1)/\beta$)

$$M_{2n} = \int_{-\infty}^{\infty} d\xi \, \xi^{2n} \psi = \frac{2N'}{\beta} \frac{\Gamma(\nu)}{\lambda^\nu}$$

$$M_{2n+1} = 0.$$ (B9)

We take $N' = \beta\lambda^{1/\beta}/2\Gamma(1/\beta)$, so that $M_0 = 1$. We can again write the density as

$$f(\xi) = \sum_{m=0}^{\infty} c_n H_n(\xi)\psi,$$

where the $H_n(\xi)$ are a set of polynomials orthogonal on $(-\infty, \infty)$, with the weight function $\psi(\xi)$, chosen so that

$$H_0 = 1,$$
$$H_1 = \xi,$$
$$H_{n+1} = \xi H_n - r_n H_{n-1}.$$ (B10)

The recurrence coefficients r_n are equal to quotients of Gram determinants, as discussed in ERDELYI et al., 1963.

The norm of the polynomials H_n is (ERDELYI et al., 1963)

$$\int d\xi \, H_n{}^2(\xi)\psi(\xi) = \prod_{i=1}^{n} r_i \int d\xi \, \psi(\xi) = \prod_{i=1}^{n} r_i.$$ (B11)

Write

$$H_n(\xi) = \sum_{m=0}^{[n/2]} h_m{}^n \xi^{n-2m};$$

from (B10) we have

$$h_m{}^n = 0, \quad m < 0 \quad \text{or} \quad m > n/2$$
$$h_0{}^n = 1$$
$$h_m{}^{n+1} = h_m{}^n - r_n h_{m-1}^{n-1},$$

so that

$$h_m{}^n = (-)^m \sum_{i_m=2m-1}^{n-1} \sum_{i_{m-1}=2m-3}^{i_m-2} \cdots \sum_{i_1=1}^{i_2-2} r_{i_m} \cdots r_{i_1}.$$ (B12)

The expression for the c_n cannot be expressed as concisely as in the gaussian case. Proceeding as before, we obtain

$$\left(\prod_{i=1}^{n} r_i\right) c_n = \alpha \sum_{m=0}^{[n/2]} h_m{}^n \alpha^{n-2m} y_{n-2m},$$ (B13)

where

$$y_n = \sum_{i=0}^{n} \binom{n}{i} (-a)^{n-i} \nu_i. \tag{B14}$$

We now have three parameters, a, β, and λa^β. λ may without loss of generality be chosen to satisfy some criterion of computational ease, but should reduce to $\lambda = \frac{1}{2}$ for $\beta = 2$; in all the calculations done here, λ was chosen so that $r_1 = 1$.

The distribution ψ_0 is unskewed, so we can not demand that $c_1 = c_3 = 0$, or, more generally, that any two odd coefficients vanish simultaneously.

The only fitting that has been done is the simplest case,

$$c_1 = c_2 = c_4 = 0.$$

These conditions are

$$c_1: \quad y_1 = 0 \tag{B15a}$$

$$c_2: \quad \alpha^2 y_2 - r_1 = 0 \tag{B15b}$$

$$c_4: \quad \alpha^4 y_4 - (r_1 + r_2 + r_3)\alpha^2 y_2 + r_1 r_3 = 0, \tag{B15c}$$

so that

$$\frac{r_2}{r_1} = \frac{y_4}{y_2^2} - 1, \tag{B16}$$

with

$$r_2/r_1 = \Gamma(1/\beta)\Gamma(5/\beta)/\Gamma^3(3/\beta), \quad \text{from (B14)}. \tag{B16a}$$

We want also the integral of f outside the target:

$$\int_{-\infty}^{0} dx\, f(x) = \frac{1}{\alpha} \int_{-\infty}^{-a\alpha} d\xi \sum_{n=0}^{\infty} c_n H_n(\xi)\psi = \frac{1}{\alpha} \sum_{n=0}^{\infty} c_n \sum_{m=0}^{[n/2]} h_m^{\,n} I_{n-2m} \tag{B17}$$

where

$$I_n = \int_{-\infty}^{-a\alpha} d\xi\, \xi^n N' e^{-\lambda|\xi|^\beta} = \frac{(-1)^n \Gamma(n+1/\beta, \lambda(a\alpha)^\beta)}{2\Gamma(1/\beta)\lambda^{n/\beta}} \tag{B17a}$$

and the Γ in the numerator is the incomplete gamma function (Abramowitz & Stegun, 1964).

APPENDIX C

Point-Source distributions

For a point source the distribution function can be studied in three dimensions. We begin by comparing moments of the distribution in various co-ordinate systems (Fig. 12). We have been calculating the moments

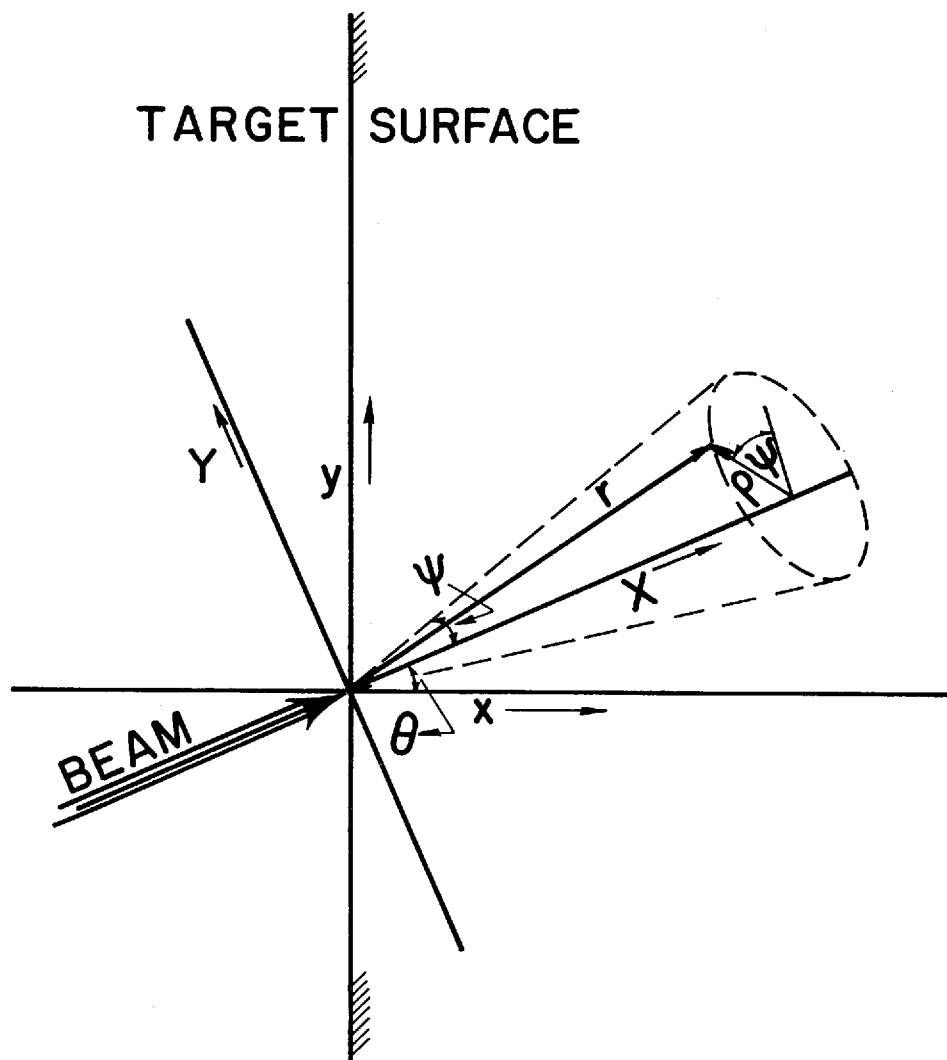$$\nu_n = \int dx\, dy\, dz\, x^n F(\vec{r}), \tag{C1}$$

Fig. 12. Plane-source and Point-source coordinates (see text).

dropping the velocity variable $\vec{v}$ for the moment. We have written (C1) as a Legendre polynomial series in the angle θ between beam and surface normal:

$$v_n = v_n(\theta) = \sum (2l + 1) A_l^n P_l(\cos \theta) = \sum_{m=0}^{[n/2]} (2n - 4m + 1) A_{n-2m}^n P_{n-2m}(\cos \theta) \quad (C2)$$

Moments in the following beam-centred coordinate systems are also used:

1) rectangular coordinates XYZ:

$$f_{n,2m,2l} = \int dX dY dZ X^n Y^{2m} Z^{2l} F(\vec{r}) \tag{C3}$$

2) cylindrical coordinates X,ϱ,ψ:

$$\omega_{n,2m} = 2\pi \int dX d\varrho\varrho X^n \varrho^{2m} F(\vec{r}) \tag{C4}$$

3) spherical coordinates r,φ,ψ:

$$f_m{}^n = 2\pi \int dr r^2 d(\cos\varphi) r^n P_m(\cos\varphi) F(\vec{r}). \tag{C5}$$

One relation is trivial:

$$f_{n,2m,2l} = \frac{\binom{2m}{m}\binom{2l}{l}}{2^{2m+2l}\binom{m+1}{m}} \omega_{n,2m+2l}. \tag{C6}$$

Another is given by BERGER and SPENCER (1959); in our notation,

$$f_{n-2m,2m,0} = \frac{1}{\binom{n}{2m}} \sum_{l=0}^{[n/2]} (2n - 4l + 1) A_{n-2l}^n \beta_{nml}. \tag{C7}$$

By similar methods one can show

$$A_{n-2m}^n = \sum_{l=0}^{[n/2]} \binom{n}{2l} f_{n-2l,2l,0} \alpha_{nml}, \tag{C8}$$

$$\omega_{n-2m,2m} = \sum_{l=0}^{[n/2]} f_{n-2l}^n (2n - 4l + 1) \alpha_{nlm} \tag{C9}$$

$$f_{n-2m}^n = \sum_{l=0}^{[n/2]} \omega_{n-2l,2l} \beta_{nlm}, \tag{C10}$$

and

$$A_{n-2m}^n = \sum_{l=0}^{[n/2]} (2n - 4l + 1) f_{n-2l}^n \sum_{k=0}^{[n/2]} \alpha_{nmk} \alpha_{nlk}, \tag{C11}$$

where we have written

$$\alpha_{nml} = 2^{n-2m} \sum_{k=0}^{k_1} \binom{l}{k} \frac{(-)^{l-k}(n-2k)!\,(n-m-k)!}{(m-k)!(2n-2m-2k+1)!} \tag{C12}$$

and

$$\beta_{nml} = \frac{1}{2^{n-2l}} \sum_{k=k_0}^{[n/2]} \binom{k}{m} \frac{(-)^{k-l}(2n-2l-2k)!}{(k-l)!(n-l-k)!(n-2k)!}, \tag{C13}$$

with k_0 equal to the larger, and k_1 the smaller, of m and l.

From these moments, for example the $\omega_{n,2j}$, we can construct the density in three dimensions, as in Fig. 11, in much the same way as was done in one dimension.

References

M. ABRAMOWITZ & I. A. STEGUN, 1964. Handbook of Mathematical Functions. Nat. Bur. Stand., Washington, D.C.

H. H. ANDERSEN, 1968. The Energy Efficiency of Lead Self-Sputtering, Appl. Phys. Letters, 13, 85.

H. H. ANDERSEN, 1970. The Sputtering Efficiency of Polycrystalline Solids. Rad. Eff. 3, 51,

E. M. BAROODY, 1964. Stopping by Elastic Collisions of Particles from a Unidirectional Plane Source. J. Appl. Phys. 35, 2074.

E. M. BAROODY, 1965. Influence of Anisotropic Scattering on Stopping by Elastic Collisions. J. Appl. Phys. 36, 3565.

E. M. BAROODY, 1969. Stopping by Elastic Collisions of Kilovolt Ions in Gaseous Mixtures and Amorphous Compounds. J. Appl. Phys. 40, 2555.

M. J. BERGER & L. V. SPENCER, 1959. General Relation Between Fluxes from Collimated Point and Plane Sources of Radiation. Phys. Rev. 113, 408.

E. BØGH, 1968. Defect Studies by Means of Channeling. Can. J. Phys. 46, 653.

N. BOHR, 1948. The Penetration of Atomic Particles Through Matter. Mat. Fys. Medd. Dan. Vid. Selsk. 18, No. 8.

D. K. BRICE, 1969. Implantation Depth Distributions: Energy Deposition into Atomic Processes and Ion Locations. Appl. Phys. Lett.. 16, 103.

F. BROWN & J. A. DAVIES, 1963. The Effect of Energy and Integrated Flux on the Retention and Range of Inert Gas Ions Injected at keV Energies in Metals. Can. J. Phys. 41, 844.

A. CORCIOVEI, G. GHIKA, & D. GRECU, 1962. La Fonction de Distribution des Atomes Déplacés dans un Solide Produits par des Irradiations. Rev. de Physique ((Bucharest) 7, 227.

A. CORCIOVEI, A. BABCENKO, & D. GRECU, 1963. Fonction de Distribution des Atomes Interstitiels et des Lacunes d'une Cascade de Déplacements produite par Irradiation. Rev. de Physique (Bucharest) 8, 445.

A. CORCIOVEI & M. CROITORU, 1966. Integral Equation for the Distribution of Interstitial Atoms of a Cascade Produced by Irradiation. Rev. Roum. Phys. 11, 317.

H. CRAMÉR, 1945. Mathematical Methods of Statistics, Princeton, University Press.

J. A. DAVIES, G. C. BALL, F. BROWN, & B. DOMEIJ, 1964. Range of Energetic ^{125}Xe Ions in Monocrystalline Silicon. Can. J. Phys. 42, 1070.

J. A. DAVIES, J. DENHARTOG, L. ERIKSSON, & J. W. MAYER, 1967. Ion Implantation of Silicon. I. Atom Location on Lattice Disorder by Means of 1.0 MeV Helium Ion Scattering. Can. J. Phys. 45, 4053.

P. H. DEDERICHS, 1965. Die räumliche Struktur einer Defektkaskade im Gasmodell. Phys. Stat. Sol. 10, 303.

P. H. DEDERICHS, G. LEIBFRIED, & K. MIKA, 1966. Näherungslösungen einer Boltzmann-Gleichung für Primäratome und Defekte. Nukleonik 8, 80.

A. ERDELYI, W. MAGNUS, F. OBERHETTINGER, & F. G. TRICOMI, 1953. Higher Transcendental Functions, Vol. II, Chapter X, McGraw-Hill, New York.

A. Erdelyi, W. Magnus, F. Oberhettinger, & F. G. Tricomi, 1954. Tables of Integral Transforms, Vol. II, McGraw-Hill, New York.

R. M. Felder & M. D. Kostin, 1966. Energy Distribution of Energetic Atoms in an Irradiated Medium. II. Single Species Case: Application to Radiation Damage Calculations. J. Appl. Phys. 37, 791.

W. Feller, 1966. An Introduction to Probability Theory and its Applications, Vol. II, Wiley, New York.

R. L. Hines & R. Arndt, 1960. Radiation Effects of Bombardement of Quartz & Vitreous Silica by 7.5 keV to 59 keV Positive Ions, Phys. Rev. 119, 623.

G. Högberg & H. Nordén, 1969a. Damage in Gold Bombarded with Medium Mass Ions. Forskningsrådens Laboratorium, Studsvik, Sweden. Unpublished Report LF-24.

G. Högberg & H. Nordén, 1969b. The Energy Dependence of Krypton Ion Damage in Gold. Phys. Stat. Sol. 33, K71.

D. K. Holmes & G. Leibfried, 1960. Range of Radiation Induced Primary Knock-ons in the Hard Core Approximation. J. Appl. Phys. 31, 1046.

R. v. Jan, 1964. Defektverteilung in Verlagerungskaskaden. I. Phys. Stat. Sol. 6, 925.

M. G. Kendall & A. Stuart, 1958. The Advanced Theory of Statistics, Vol. I, Griffin, London.

M. D. Kostin, 1965. Energy Distribution of Energetic Atoms in an Irradiated Medium. J. Appl. Phys. 36, 850.

C. Lehmann, 1961. Zur Bildung von Defektkaskaden in Kristallen beim Beschuss mit energiereichen Teilchen. Nukleonik 3, 1.

G. Leibfried, 1962. Calculation of Averages for Primary Recoil Distributions. J. Appl. Phys. 33, 1933.

G. Leibfried, 1963. Higher Order Averages of Primary Recoil Distributions. Z. Physik 171, 1.

G. Leibfried & K. Mika, 1965. Boltzmann-Gleichungen für die Verteilung von Primäratomen. Nukleonik 7, 309.

J. Lindhard & M. Scharff, 1961. Energy Dissipation by Ions in the keV Region, Phys. Rev. 124, 128.

J. Lindhard, V. Nielsen, M. Scharff, & P. V. Thomsen, 1963a. Integral Equations Governing Radiation Effects (Notes on Atomic Collisions III). Mat. Fys. Medd. Dan. Vid. Selsk. 33, No. 10.

J. Lindhard, M. Scharff, & H. E. Schiøtt, 1963b. Range Concepts & Heavy Ion Ranges (Notes on Atomic Collisions II). Mat. Fys. Medd. Dan. Vid. Selsk. 33, No. 14.

J. Lindhard, V. Nielsen, & M. Scharff, 1968. Approximation Method in Classical Scattering by Screened Coulomb Fields (Notes on Atomic Collisions I). Mat. Fys. Medd. Dan. Vid. Selsk. 36, No. 10.

R. J. MacDonald & D. Haneman, 1966a. Depths of Low-Energy Ion Bombardment Damage in Germanium. J. Appl. Phys. 37, 1609.

R. J. MacDonald & D. Haneman, 1966b. Low-Energy-Ion-Bombardment Damage in Germanium. J. Appl. Phys. 37, 3048.

J. W. Mayer, L. Eriksson, S. T. Picraux, & J. A. Davies, 1968. Ion Implantation of Silicon & Germanium at Room Temperature. Analysis by Means of 1.0 – MeV Helium Ion Scattering. Can. J. Phys. 46, 663.

J. W. MAYER, L. ERIKSSON, & J. A. DAVIES, 1969. Ion Implantation of Semi-conductors; Academic Press, New York

J. W. MAYER & O. J. MARSH, 1969. Ion Implantation in Semiconductors, Applied Solid State Science **1**, 239.

K. L. MERKLE, 1966. Radiation-Induced Point Defect Clusters in Copper & Gold. I. Clusters Produced in Energetic Displacement Cascades, Phys. Stat. Sol. **18**, 173.

K. O. NIELSEN, 1956. The Range of Atomic Particles with Energies about 50 keV, in "Electromagnetically Enriched Isotopes & Mass Spectrometry", Acad. Press, New York, p. 68.

D. I. R. NORRIS, 1969. Depth Distributions of Vacancy Clusters in Ion Bombarded Gold & Nickel. Phil. Mag. **19**, 653.

O. S. OEN, D. K. HOLMES, & M. T. ROBINSON, 1963. Ranges of Energetic Atoms in Solids, J. Appl. Phys. **34**, 302.

O. S. OEN & M. T. ROBINSON, 1964. Monte Carlo Range Calculations for a Thomas-Fermi Potential, J. Appl. Phys. **35**, 2515.

J. R. PARSONS, 1965. Conversion of Crystalline Germanium to Amorphous Germanium by Ion Bombardment. Phil. Mag. **12**, 1159.

J. R. PARSONS & R. W. BALLUFFI, 1964. Displacement Spike Crystallization of Amorphous Germanium during Irradiation. J. Phys. Chem. Solids **25**, 263.

P. V. PAVLOV, D. I. TETEL'BAUM, E. I. ZORIN, & V. I. ALEKSEEV, 1966. Distribution of Implanted Atoms and Radiation Defects in the Ion Bombardment of Silicon (Monte Carlo Method). Fizika Tverdogo Tela **8**, 2679 (Engl. Transl. in Sov. Phys. Solid State **8**, 2141 (1967)).

J. S. PRINGLE, 1968. Private Communication.

M. T. ROBINSON, 1965a. The Influence of the Scattering Law on the Radiation Damage Displacement Cascade. Phil. Mag. **12**, 741.

M. T. ROBINSON, 1965b. The Energy Spectra of Atoms Slowing Down in Structure-less Media. Phil. Mag. **12**, 145.

J. B. SANDERS, 1966. Recoil Numbers in Crystalline Structures. Physica **32**, 2197.

J. B. SANDERS, 1968a. Ranges of Projectiles in Amorphous Materials. Can. J. Phys. **46**, 455.

J. B. SANDERS, 1968b. On Penetration Depths & Collision Cascades in Solid Materials. Thesis, University of Leiden.

J. B. SANDERS, 1969. On the Spatial Distribution of Recoil Atoms, Created in a Collision Cascade in Crystalline Material. Physica **41**, 353.

L. I. SCHIFF, 1955. Quantum Mechanics, McGraw-Hill, New York.

H. E. SCHIØTT, 1966. Range-Energy Relations for Low-Energy Ions. Mat. Fys. Medd. Dan. Vid. Selsk. **35**, No. 9.

H. E. SCHIØTT, 1968. Projected Ranges of Light Ions in Heavy Substances. Can. J. Phys. **46**, 449.

P. SIGMUND & J. B. SANDERS, 1967. Spatial Distribution of Energy Deposited by Ionic Bombardment. Proc. Int. Conf. on Application of Ion Beams to Semi-conductor Technology, ed. P. GLOTIN, Editions Ophrys, p. 215.

P. SIGMUND, G. P. SCHEIDLER, & G. ROTH, 1968. Spatial Distribution of Defects in Cascades. Black Spot Defects in Electron-Bombarded Copper. Proc. Conf. on "Solid State Research with Accelerators", ed. A. N. GOLAND, BNL-50083 (C-52), p. 374.

P. SIGMUND, 1968. Sputtering Efficiency of Amorphous Substances. Can. J. Phys. **46**, 731.

P. Sigmund, 1969a. Theory of Sputtering I. Sputtering Yield of Amorphous & Polycrystalline Targets. Phys. Rev. **184**, 383.

P. Sigmund, 1969b. A Note on Integral Equations of the Kinchin-Pease Type. Rad. Eff. **1**, 15.

P. Sigmund, 1969c. On the Number of Atoms Displaced by Implanted Ions or Energetic Recoil Atoms. Appl. Phys. Letters, **14**, 114.

L. E. Thomas, T. Schober, & R. W. Balluffi, 1969. Defects Observed by Electron Microscopy in Gold Bombarded with Gold Ions. I–III. Rad. Eff. **1**, 257, 269, & 279.

K. B. Winterbon, 1970. To be published.

K. B. Winterbon*
Chalk River Nuclear Laboratories
Chalk River, Ontario, Canada.

Peter Sigmund†*
Argonne National Laboratory
Argonne, Illinois, U.S.A.

J. B. Sanders*
F.O.M. Institute for Atomic & Molecular Physics
Amsterdam, Netherlands.

† Work performed under the auspices of the U.S. Atomic Energy Commission.
* Present address: Institute of Physics, University of Aarhus, Denmark.